

**DAHLGREN DIVISION
NAVAL SURFACE WARFARE CENTER**

Dahlgren, Virginia 22448-5100



NSWCDD/TR-96/227

**MECHANICAL ANALYSES SUPPORTING THE
DESIGN OF A HEAVY-WALLED TOMAHAWK
CONCENTRIC CANISTER LAUNCHER**

**BY JOHN W. POWERS RICHARD H. SETTLE
WEAPONS SYSTEMS DEPARTMENT**

MAY 1997

DTIC QUALITY INSPECTED 2

Approved for public release; distribution is unlimited.

19970620 006

REPORT DOCUMENTATION PAGE

Form Approved
OMB No. 0704-0188

Public reporting burden for this collection of information is estimated to average 1 hour per response, including the time for reviewing instructions, search existing data sources, gathering and maintaining the data needed, and completing and reviewing the collection of information. Send comments regarding this burden or any other aspect of this collection of information, including suggestions for reducing this burden, to Washington Headquarters Services, Directorate for information Operations and Reports, 1215 Jefferson Davis Highway, Suite 1204, Arlington, VA 22202-4302, and to the Office of Management and Budget, Paperwork Reduction Project (0704-0188), Washington, DC 20503.

1. AGENCY USE ONLY (Leave blank)	2. REPORT DATE May 1997	3. REPORT TYPE AND DATES COVERED Final	
4. TITLE AND SUBTITLE Mechanical Analyses Supporting The Design of a Heavy-Walled Tomahawk Concentric Canister Launcher		5. FUNDING NUMBERS	
6. AUTHOR(s) John W. Powers, Richard H. Settle		8. PERFORMING ORGANIZATION REPORT NUMBER NSWCDD/TR-96/227	
7. PERFORMING ORGANIZATION NAME(S) AND ADDRESS(ES) Commander Naval Surface Warfare Center Dahlgren Division (Code G72) 17320 Dahlgren Road Dahlgren, VA 22448-5100		10. SPONSORING/MONITORING AGENCY REPORT NUMBER	
9. SPONSORING/MONITORING AGENCY NAME(S) AND ADDRESS(ES)		11. SUPPLEMENTARY NOTES	
12a. DISTRIBUTION/AVAILABILITY STATEMENT Approved for public release; distribution is unlimited.		12b. DISTRIBUTION CODE	
13. ABSTRACT (Maximum 200 words) Structural calculations used to support the design of a heavy-walled Concentric Canister Launcher to withstand a Tomahawk restrained firing are summarized. The loads on the components arise from internal pressure, temperature, and the motor thrust. These loads are used to size components and to predict factors of safety. The test canister is over-designed for the thrust and pressure loads. The largest concern is the thermal loads on the structure. High thermal stresses may cause localized yielding in the lower portion of the uptake. Additionally, localized "hot spots" not accounted for in one-dimensional fluids calculations have the potential to erode or melt the structure.			
14. SUBJECT TERMS Concentric Canister Launcher, restrained firing, Mk 10 assembly, uptake assembly, plenum assembly, load conditions, internal pressure, Mises stress			15. NUMBER OF PAGES 46
			16. PRICE CODE
17. SECURITY CLASSIFICATION OF REPORTS UNCLASSIFIED	18. SECURITY CLASSIFICATION OF THIS PAGE UNCLASSIFIED	19. SECURITY CLASSIFICATION OF ABSTRACT UNCLASSIFIED	20. LIMITATION OF ABSTRACT UL

FOREWORD

The mechanical analyses presented here were used to help size a heavy-walled Concentric Canister Launcher (CCL). Along with the calculations presented here, Naval Surface Warfare Center, Dahlgren Division (NSWCDD) Code G72 Computational Fluid Dynamics personnel performed analyses to help size the uptakes. The drawings of the heavy-walled CCL were made by Richard Settle of the Computer Aided Engineering Technology Branch. The launcher is scheduled to be tested early in 1997.

The work presented here was funded by the Concentric Canister Launcher program office via the Office of Naval Research.

This report has been reviewed by R.W. Mattozzi, Head of the Weapons Integration and Technology Branch, and G.C. Blount, Head of the Combat Systems Safety and Engineering Division.

Approved by:



DAVID S. MALYEVAC, Deputy Head
Weapons Systems Department

CONTENTS

<u>Chapter</u>	<u>Page</u>
1 INTRODUCTION	1
2 MECHANICAL PERFORMANCE OF UPTAKE AND PLENUM UNDER INTERNAL PRESSURES AND TEMPERATURES	7
2.1 LOAD CONDITIONS	7
2.2 ANALYSES OF THE UPTAKE	8
2.3 ANALYSIS OF THE PLENUM	18
3 RESTRAINT OF THE MK 106 BOOSTER	25
3.1 BACKGROUND	25
3.2 RESTRAINING THE MK 106 IN THE MK 10 CANISTER	25
3.3 RESTRAINING THE MK 10 IN THE CCL	27
4 SUMMARY AND RECOMMENDATIONS	35
4.1 SUMMARY	35
4.2 GENERAL RECOMMENDATIONS	36
4.3 RECOMMENDATIONS TO REDUCE THE PLENUM WEIGHT	36
4.4 RECOMMENDATIONS TO REDUCE THE UPTAKE WEIGHT	38
5 REFERENCES	39
DISTRIBUTION	(1)

ILLUSTRATIONS

<u>Figure</u>	<u>Page</u>
1 HEAVY-WALLED CONCENTRIC CANISTER LAUNCHER	2
2 SUB-ASSEMBLIES OF HEAVY-WALLED CCL	3
3 UPTAKE ASSEMBLY	4
4 PLENUM ASSEMBLY	5
5 UPTAKE FINITE ELEMENT MESH	9

ILLUSTRATIONS (Continued)

<u>Figure</u>		<u>Page</u>
6	VON MISES STRESSES IN UPTAKE UNDER 14.4 PSIG UNIFORM PRESSURE	13
7	MODE SHAPE FOR BUCKLING OF THE UPTAKE	15
8	PLENUM FINITE ELEMENT MESH	19
9	VON MISES STRESSES IN PLENUM UNDER 100 PSIG UNIFORM PRESSURE	20
10	VON MISES STRESSES IN PLENUM UNDER 100 PSIG UNIFORM PRESSURE (WITH TOP FLANGE REMOVED)	21
11	MK 10 ASSEMBLY	26
12	EULER BEAM MODEL USED FOR BUCKLING ANALYSIS	27
13	LOWER RESTRAINTS FOR MK 106 AND MK 10	28
14	DISPLACEMENTS IN INNER CYLINDER BASEPLATE UNDER THRUST LOAD	31
15	VON MISES STRESSES IN INNER CYLINDER BASEPLATE UNDER THRUST LOAD	33

TABLES

<u>Table</u>		<u>Page</u>
1	ROOM TEMPERATURE MECHANICAL PROPERTIES OF ASTM A387 GR 22 CLASS 1 PLATES	8
2	PEAK MISES STRESSES IN UPTAKE UNDER 80 PSIG INTERNAL PRESSURE	10
3	PEAK MISES STRESSES IN UPTAKE UNDER 20 PSIG INTERNAL PRESSURE	11
4	PEAK MISES STRESSES IN UPTAKE UNDER 14.4 PSIG INTERNAL PRESSURE USED TO SIMULATE THE TRANSIENT PULSE	11
5	PEAK MISES STRESSES IN UPTAKE UNDER 2 PSIG INTERNAL PRESSURE USED TO SIMULATE THE STEADY STATE PRESSURE ...	12
6	PROPERTIES OF ASTM A387 GR 22 CLASS 2 PLATES AT 300°F AND 1100°F	17
7	PEAK MISES STRESSES IN PLENUM UNDER 80 PSIG INTERNAL PRESSURE	22
8	PEAK MISES STRESSES IN PLENUM UNDER 40 PSIG INTERNAL PRESSURE	22
9	ESTIMATED WEIGHTS OF HEAVY-WALLED CCL COMPONENTS ...	36

CHAPTER 1

INTRODUCTION

The design of the Concentric Canister Launcher (CCL) for the first Tomahawk restrained firing was conducted in a very short time. The emphasis was not placed on obtaining an optimized design, but rather on obtaining a conservative design that could withstand a Mk 106 restrained firing. As a result, what is termed a heavy-walled test canister was produced. The information from this test will then be used to design a more optimized prototype.

In keeping with the pace dictated by the test schedule, the structural calculations used to support the design consist of closed-form solutions reinforced by finite element analyses as needed. Throughout, an attempt has been made to balance the level of detail of the analyses with the time constraints. Typically, this has been accomplished by making conservative assumptions and using large factors of safety. In many cases, components had to be designed using engineering experience. Then they were checked analytically later, as time permitted.

The heavy-walled CCL is shown in Figure 1. It consists of three primary assemblies: a Mk 10 assembly, an uptake assembly, and a plenum assembly. These assemblies are labeled in Figure 2. The Mk 10 assembly consists of a shortened Mk 10 canister that houses the Mk 106 booster. It is bolted in the uptake assembly through a flange at the top and separation nuts at the bottom. The uptake assembly is shown in Figure 3. It consists of two concentric canisters held in place by four longerons, or webs. It holds the Mk 10 assembly in place and vents the exhaust gases out of the launcher. The plenum assembly bolts onto the bottom of the uptake assembly and turns the flow up into the uptake. This assembly is drawn in Figure 4. The plenum is octagonal so that standard flat ablative panels could be used. Curved panels that would be needed for a cylindrical or hemispherical shape would need to be custom made and would require a great deal of additional time and money. A more detailed description of all these components can be found in Reference 1 and in the drawing package for the canister.

The structure was designed using two different loading scenarios. The first scenario uses internal pressures and temperatures from the motor exhaust. The diameters and wall thicknesses of the cylinders that form the uptake were determined using wall temperatures predicted from 1-dimensional computational fluid dynamics, or CFD, analyses (Reference 2). The rest of the launcher was then sized around these dimensions. Additionally, experience with erosion on flat plates and in the Mk 41 Vertical Launching System helped determine the amount of ablative that was going to be used in the plenum. The mechanical analysis of the uptake considers both pressure loads and thermal stresses caused by temperature gradients in the metal. The plenum is analyzed using only pressures. It is ablated so that high temperatures should not affect the steel walls until after the burn.

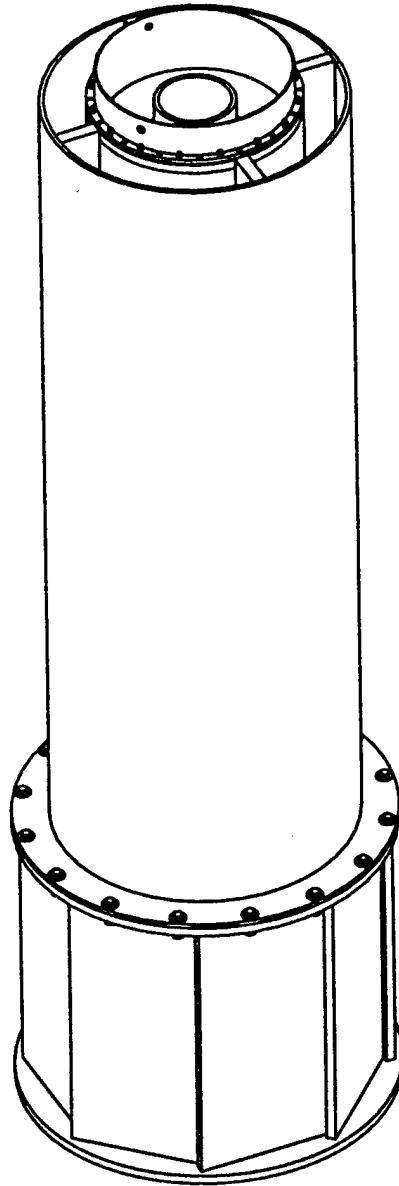


FIGURE 1. HEAVY-WALLED CONCENTRIC CANISTER LAUNCHER

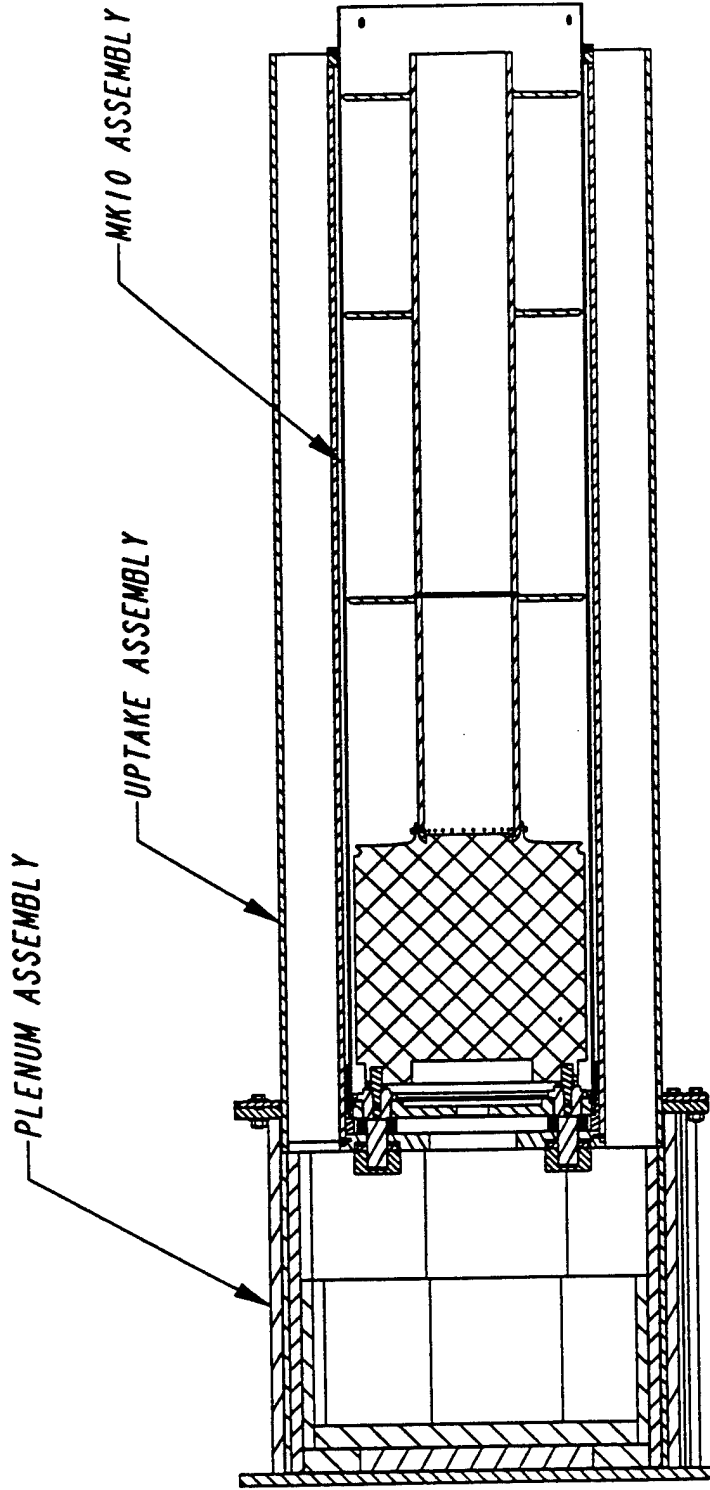


FIGURE 2. SUB-ASSEMBLIES OF HEAVY-WALLED CCL

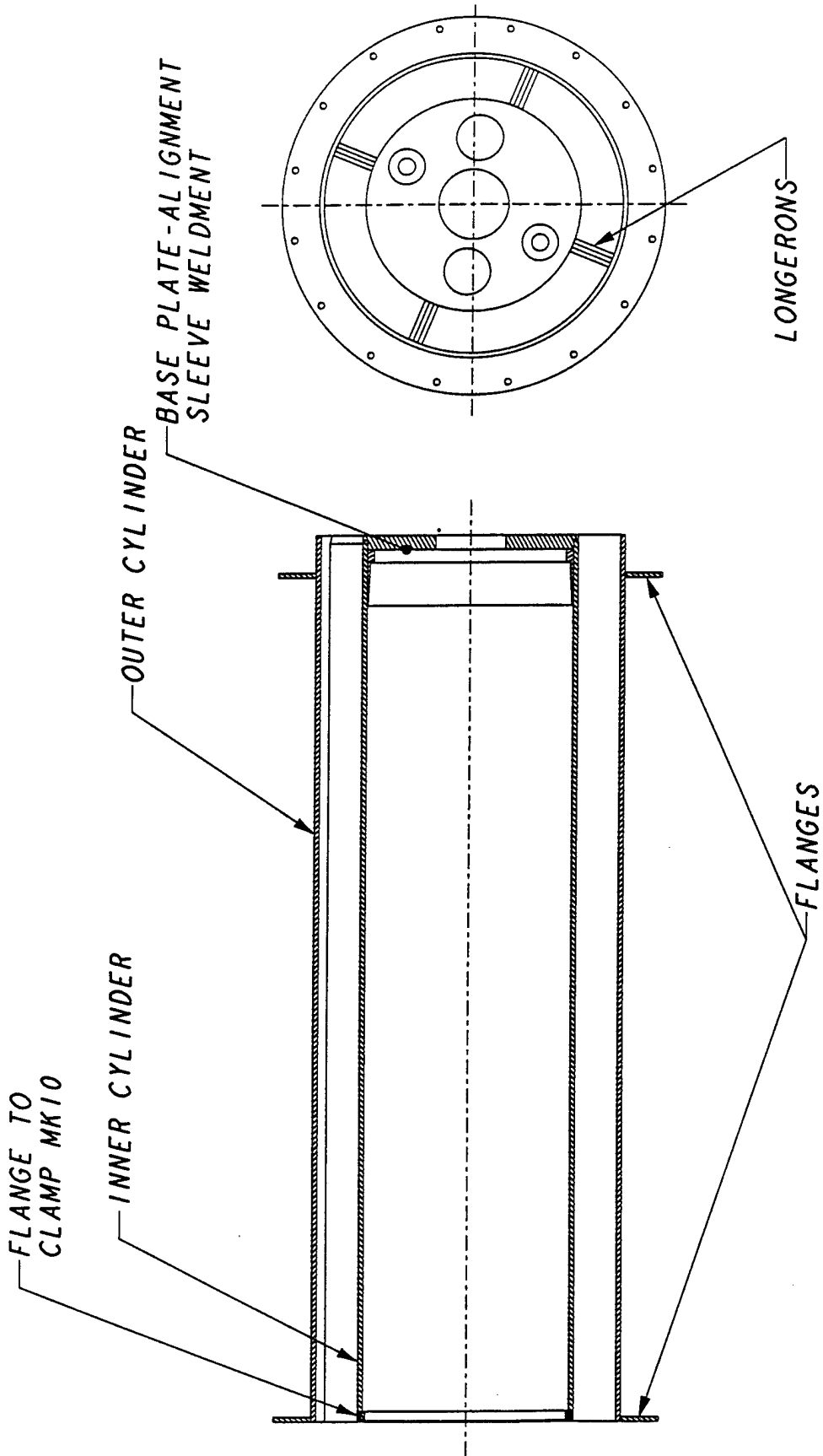


FIGURE 3. UPTAKE ASSEMBLY

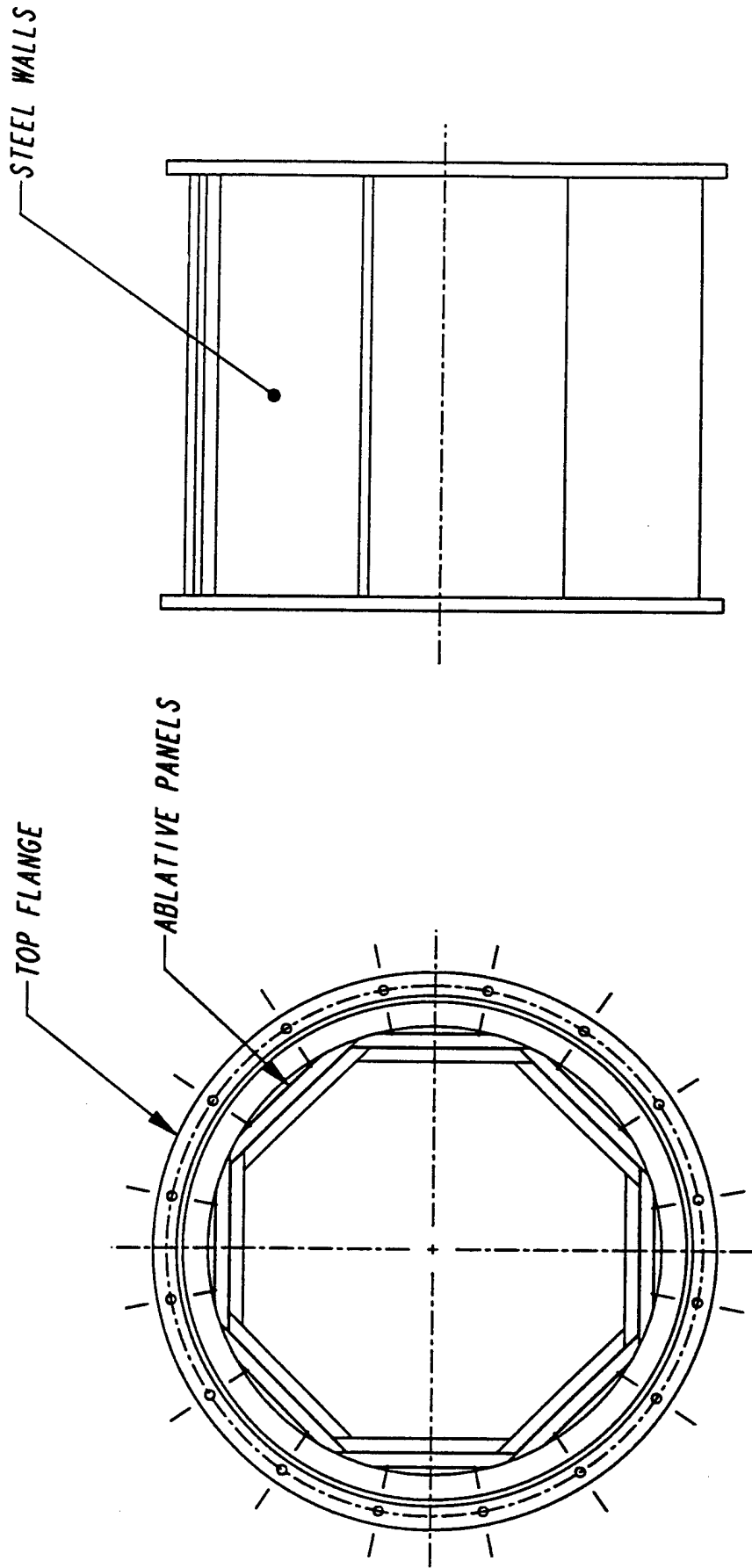


FIGURE 4. PLENUM ASSEMBLY

The second load case uses the forces caused by the rocket motor thrust. The structure of the CCL needs to be able to restrain the motor. These restraints consist of primary restraints and back-up restraints. They have been designed to be redundant so that if any were to fail, the motor would still be held in place.

CHAPTER 2

MECHANICAL PERFORMANCE OF UPTAKE AND PLENUM UNDER INTERNAL PRESSURES AND TEMPERATURES

2.1 LOAD CONDITIONS

During the restrained firing, the hot gases from the Mk 106 will flow into the plenum and then up through the uptake. The steel in the uptake is unablated and must withstand both the pressures and the temperatures from the hot exhaust gas. The uptake is analyzed considering internal pressures. Both room temperature and elevated temperature material properties are used in these calculations. Additionally, an attempt has been made to predict the magnitude of thermal stresses in the steel in the uptake. The plenum has a thick layer of ablative that will insulate the steel structure from most of the heat during the restrained firing. As a result, the plenum only needs to be analyzed under internal pressure loads.

As already mentioned, the uptake is sized using the results of one-dimensional CFD calculations. These calculations predict that a CCL with an unablated uptake can withstand a Mk 106 restrained firing if the uptake has an inner diameter of 21.84 in., an outer diameter of 29.5 in., and 1/4 in. thick steel walls (Reference 2). The radial dimensions of the entire canister were sized around these calculations.

In an attempt to remain conservative for this test, the outside diameter of the uptake was increased from 29.5 in. to 32 in. and the wall thickness was doubled, from 1/4 in. thick to 1/2 in. thick. Additionally, the inner diameter of the uptake needed to be increased to 23 in. to better hold the Mk 10 canister. One-dimensional CFD calculations using these new dimensions resulted in a peak temperature of 2150°F in the steel at the entrance to the uptake (Reference 3). The back wall temperature at this location is predicted to be only 500°F. The temperature rapidly decreases up the uptake. At the top of the uptake, the peak surface temperature is 700°F and the back wall temperature is only 200°F. The peak pressure at the entrance of the uptake is expected to be 7.2 psig during the initial transient pulse and only 2 psig during the steady-state portion of the burn. As with the temperatures, the pressures decrease up the uptake. Both the peak transient pulse and the steady state pressures are predicted to be less than 1 psig at 94 in. up the uptake. (The uptake is 96 in. long.) Nevertheless, the peak pressures of 7.2 psig for the initial transient pulse and 2 psig for the steady state burn will be applied the entire length of uptake for the following analyses. It is important to realize that the walls will still be at ambient temperature when the higher-pressure transient pulse hits. As the walls get hot and material properties degrade, they will only have to withstand a maximum of 2 psig internal pressure.

Both the uptake and the plenum are made from ASTM A387 grade 22 class 2 pressure vessel plates. This is a 2.25Cr-1Mo alloy steel. The room temperature properties of A387 Gr 22 class 2 plates are listed in Table 1. This material was chosen because it is widely used for elevated temperature service in the pressure vessel industry. So, besides maintaining strength at elevated temperatures, A387 Gr 22 can be acquired in a short time and at a reasonable cost.

TABLE 1. ROOM TEMPERATURE MECHANICAL PROPERTIES OF ASTM A387 GR 22 CLASS 1 PLATES

Property	Value
Elastic Modulus, E	30 Msi
Poisson's Ratio, ν	0.26
Density, ρ	0.283 lbm/in ³
Ultimate Tensile Strength, Su	75 ksi
Yield Strength, Sy	45 ksi

2.2 ANALYSES OF THE UPTAKE

The uptake is analyzed considering internal pressures during both the test event and a planned hydrotest. This is accomplished using a finite element model. A stability analysis is also performed to ensure the inner cylinder of the uptake will not buckle under the internal pressures. Finally, thermal stresses are checked using closed-form solutions.

2.2.1 Internal Pressure in the Uptake

A finite element analysis is used to evaluate the mechanical response of the uptake to internal pressures. The first model simulates the uptake hydrotest configuration. In the hydrotest, the top of the uptake will be capped with a plate and the bottom will be connected to the plenum. The bottom of the inner cylinder will be closed with a solid plate so that only the inside of the uptake will be pressurized. A uniform internal pressure is applied inside the uptake and against the top cover and the plenum. Under this uniform loading, the stresses that are predicted will be proportional to the internal pressure as long as stresses remain below the yield strength of the material. Once stresses are calculated at one pressure, they can be determined at any other pressure of interest.

The finite element model is created using Patran as a pre- and post-processor and the analysis is conducted using Abaqus. Figure 5 shows the model used. It consists of 1/4 of an inner cylinder that is connected to 1/4 of an outer cylinder by a longeron using 8-node quadratic shell elements. Symmetric boundary conditions are used along the straight edges of the curved plates. The two curved plates are both 1/2 in. thick and the longeron is 1.5 in. thick. A 1.5 in. thick base plate is also included at the bottom of the inner cylinder. The connection to the plenum is modeled by fixing the

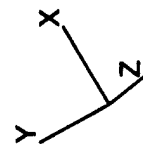
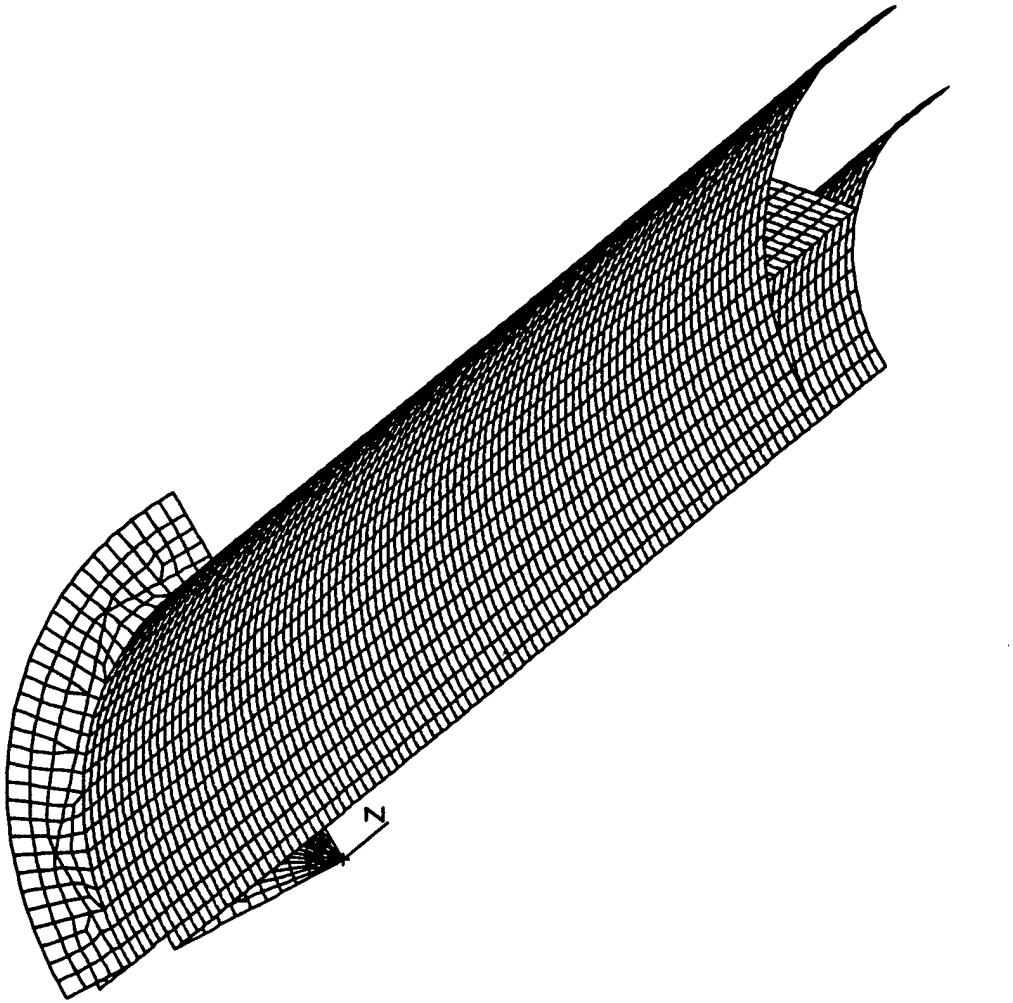


FIGURE 5. UPTAKE FINITE ELEMENT MESH

nodes in the lower flange of the uptake where the bolts are located. At the top of the uptake opening is a cover plate that will be used to hold the pressure in the uptake during the hydrotest. This plate has been omitted for clarity in Figure 5.

The inside of the uptake, the top cover plate, and the base plate are loaded by a uniform pressure. The uptake was originally going to be tested to 80 psig. The 80 psig case is included here because the stresses under a 20 psig pressure will be proportional to those under the 80 psig pressure. Thus, the analysis uses an 80 psig internal pressure. Later, this requirement was reduced to 20 psig. Under an 80 psig internal pressure, the peak predicted von Mises stress in the structure is 83.3 ksi and occurs at a node that has been fixed in the lower flange. This was expected because fixing the nodes at the bolt locations imposes an overly severe boundary condition. As a result, this stress is probably overstated. The peak Mises stresses, σ_{Mises} , predicted for each component in the uptake assembly are listed in Table 2 under an 80 psig internal pressure. Factors of safety are also included in this table using a yield strength of 45 ksi for the A387 Grade 22 steel. The factor of safety, F.S., is calculated by dividing the yield strength of the material by the stress. Factors of safety greater than 1 indicate the material can withstand the stresses.

TABLE 2. PEAK MISES STRESSES IN UPTAKE UNDER 80 PSIG INTERNAL PRESSURE

Component	σ_{Mises} (ksi)	F.S. (Using $S_y = 45$ ksi)
Flange	83.4	0.54
Outer Cylinder	48.6	0.93
Inner Cylinder	80.3	0.56
Webs	14.4	3.1
Base Plate	22.8	2.0
Cover Plate	53.6	0.84

The stresses in several components of the uptake are above the yield strength of the steel. Because of this analysis, the hydrotest was reduced to 20 psig to produce factors of safety greater than 2 for the hydrotest. This will still be nearly 3 times the peak transient pressure of 7.2 psig during the restrained firing and 10 times the steady state pressure of 2 psig. Recomputing the Mises stresses in the uptake under a 20 psig pressure gives the results listed in Table 3. Reducing the hydrotest pressure to 20 psig results in factors of safety greater than 2 for the hydrotest.

The pressures will be much lower during the restrained firing test than in the hydrotest. The pressure consists of a short-duration transient pressure spike followed by a longer duration steady-state pressure. The transient pulse has a peak predicted pressure of 7.2 psig. Since this pulse is suddenly applied, a dynamic load factor of 2 is multiplied with this pressure. Using this dynamic load factor, a static analysis is used to predict the peak stresses under a transient load. With a dynamic load factor of 2, the stresses under the transient pressure are computed by applying a 14.4 psig static

TABLE 3. PEAK MISES STRESSES IN UPTAKE UNDER 20 PSIG INTERNAL PRESSURE

Component	σ_{Mises} (ksi)	F.S. (Using $S_y = 45$ ksi)
Flange	20.8	2.1
Outer Cylinder	12.2	3.7
Inner Cylinder	20.1	2.2
Webs	3.6	12.0
Base Plate	5.7	7.9
Cover Plate	13.4	3.3

pressure. Admittedly, a dynamic load factor of 2 is a somewhat conservative assumption. The duration of the spike is so short the structure probably won't have time to fully respond before the pressure is gone. In future analyses, time needs to be allotted to conduct a transient analysis.

The hydrotest finite element model was modified to create the model used to simulate pressures during the restrained firing. The cap at the end of the uptake has been removed in this model. This significantly reduces the axial stresses in the uptake. The peak Mises stresses predicted in the uptake for the transient pulse are listed in Table 4. The highest stress is only 854 psi and occurs in the outer cylinder of the uptake. The inner cylinder has a peak predicted stress of only 682 psi. These low stresses result in margins of safety of more than 50 in all components.

TABLE 4. PEAK MISES STRESSES IN UPTAKE UNDER 14.4 PSIG INTERNAL PRESSURE USED TO SIMULATE THE TRANSIENT PULSE

Component	σ_{Mises} (ksi)	F.S. (Using $S_y = 45$ ksi)
Outer Cylinder	0.854	52
Inner Cylinder	0.682	65
Webs	0.389	115
Lower Flange	0.789	56
Upper Flange	0.750	60

The approximate magnitudes of the stresses in the cylinders are checked using simple closed form solutions. If the effects of the webs are neglected, the stress in the cylinders can be approximated using the relation

$$\sigma = \frac{pr}{t} \quad (1)$$

where p is the internal pressure, r is the average radius of the cylinder, and t is the wall thickness. The outer cylinder has an average radius of 16.25 in. and a wall thickness of 0.50 in. This results in a stress of 468 psi, a little over half the value predicted by the finite element model. Similar results are obtained for the inner cylinder. It has an average radius of 11.25 in. and a wall thickness of 0.5 in. This results in an average stress of 324 psi being predicted.

The differences between the finite element and closed-form solutions are explained by noting that the high stresses in the finite element model occur near the webs. This is shown in a plot of the Mises stresses in the outer cylinder in Figure 6. The highest stresses occur because the webs restrain the cylinder from deforming outward in response to the internal pressures. This creates localized regions of high stress. Away from the webs, the stresses drop significantly.

The unablated steel walls of the uptake will get very hot during the steady-state portion of the motor burn. The entrance of the uptake is predicted to be at 2150°F at the surface of the metal and 500°F at the back wall. This gives an average temperature of 1325°F. Data for 2.25Cr-1Mo steel is readily available only to 1200°F. As a result, material properties will be used for 1200°F 2.25Cr-1Mo steel. At this temperature, the elastic modulus is 22.5 Msi and Poisson's ratio is 0.314 (Reference 4). For normalized and tempered 2.25Cr-1Mo steel, the yield and ultimate strengths at 1200°F are 20 ksi and 30 ksi, respectively (Reference 5).

Using the same finite element model as used for the transient case and changing the elastic properties gives the Mises stresses listed in Table 5 under a steady state pressure of 2 psig. The stresses predicted are essentially negligible and result in factors of safety that are extremely large. During this portion of the burn the greatest risk to the uptake will be caused by melting and erosion, especially if there are any concentrated flows not accounted for in the 1-D CFD analysis.

TABLE 5. PEAK MISES STRESSES IN UPTAKE UNDER 2 PSIG INTERNAL PRESSURE USED TO SIMULATE THE STEADY STATE PRESSURE

Component	σ_{Mises} (ksi)	F.S. (Using $S_y = 20$ ksi for 1200°F material)
Outer Cylinder	0.119	168
Inner Cylinder	0.096	208
Webs	0.056	357
Lower Flange	0.106	188
Upper Flange	0.111	180

2.2.2 Buckling of the Uptake

As an additional check on the strength of the uptake under internal pressure, a buckling check is performed. Buckling is a concern in the design of CCL because the inner cylinder is loaded by an

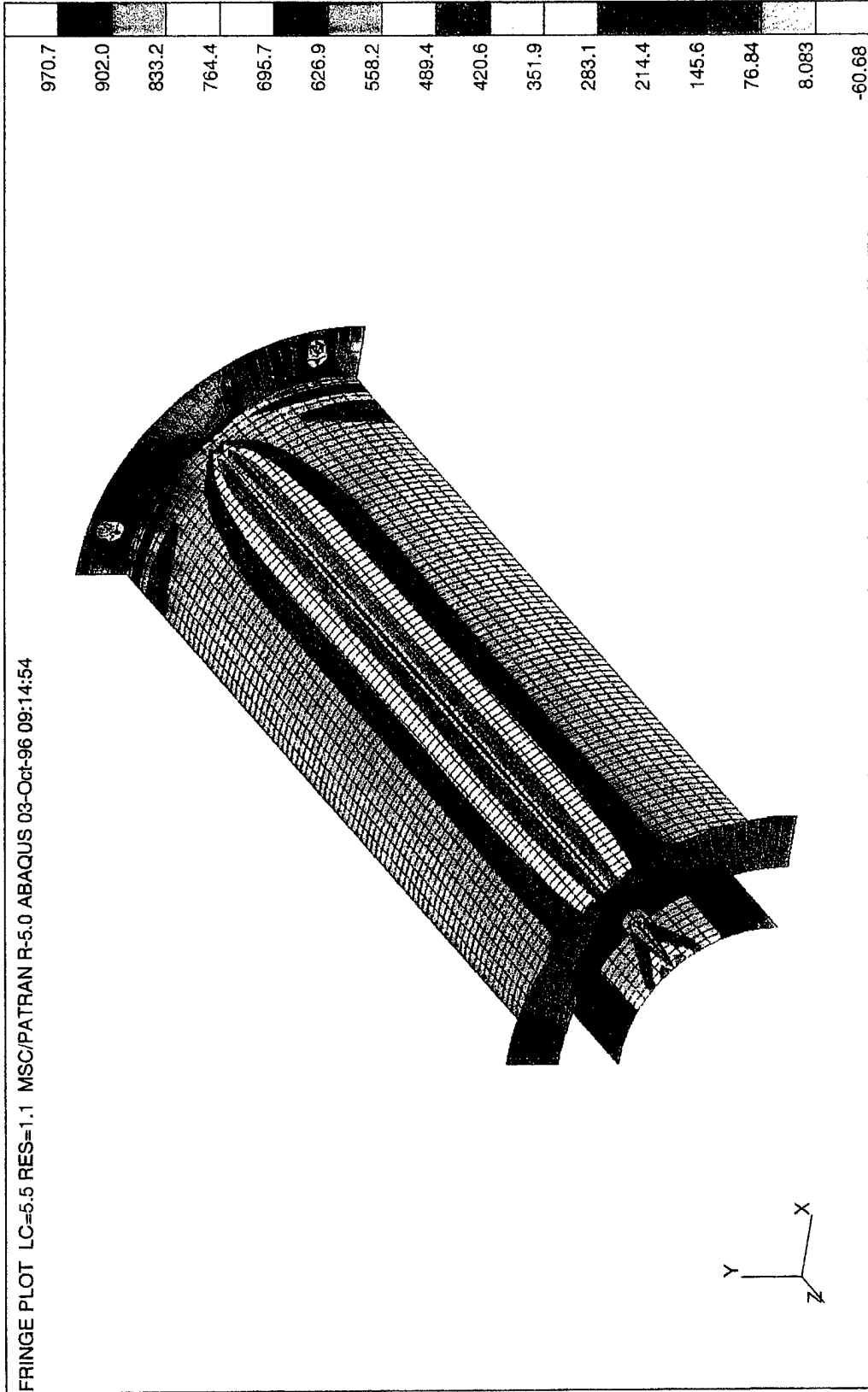


FIGURE 6. VON MISES STRESSES IN UPTAKE UNDER 14.4 PSIG UNIFORM PRESSURE

external pressure. This puts the inner cylinder in compression and makes it susceptible to buckling. The purpose of this check is to find the critical internal pressure, p_{cr} , that will cause buckling of the inner cylinder. The pressures in the uptake during the hydrotest and during the restrained firing must be below p_{cr} to prevent buckling.

Both closed-form and finite element solutions are used. The closed-form solution is expected to give conservative results (low values of p_{cr}) because the long webs connecting the inner and outer cylinder are not represented. These webs will greatly stiffen the structure and increase the buckling strength.

The closed-form solution models a cylindrical tube of length L with its ends held circular. It is loaded by a uniform external pressure. From Reference 6, the critical pressure that will cause buckling of the cylinder is

$$p_{cr} = 0.807 \frac{Et^2}{Lr} \sqrt[4]{\left[\frac{1}{(1-\nu^2)}\right]^3 \frac{t^2}{r^2}} \quad (2)$$

In this expression, E is the elastic modulus (30 Msi), L is the length of the cylinder (94.35 in.), r is the radius (11.25 in.), t is the wall thickness (0.50 in.), and ν is Poisson's ratio (0.26). The pressure that will cause this cylinder to buckle, then, is 1267 psig. This is well above the 20 psig hydrostatic pressure and the 14.4 psig transient pressure.

The buckling strength is also checked using a finite element model. The same finite element model that was used to evaluate stresses in the uptake under internal pressures during the restrained firing test is used to perform the buckling check here. The only differences are that a full model is used instead of a quarter symmetry model and the entire lower flange is restrained in the axial direction. The result of the analysis gives a critical pressure of 1884 psig. This is over 50 percent greater than predicted by the closed-form model that did not have the webs. The deflected shape of the inner canister during buckling is shown in Figure 7. (Note that the outer cylinder has been omitted for clarity.) The cylinder buckles inward at the top of the cylinder. The bottom of the inner cylinder is restrained by the large base plate and barely moves. The internal pressure during the restrained firing is only predicted to be 14.4 psig if a dynamic load factor of 2 is still used. This result gives a factor of safety of 130 for buckling.

For completeness, the finite element analysis has been conducted using 1200°F steel properties to simulate the steady-state burn. The elastic modulus is reduced to 22.5 Msi and Poisson's ratio is 0.314. Here, p_{cr} equals 1424 psig. Thus, the softer material properties reduced the buckling strength by approximately 25 percent. The metal will only be hot during the steady state portion of the burn. The pressures in the uptake are only predicted to be 2 psig during this time. As a result, a factor of safety of 712 is predicted for buckling during the steady state portion of the burn.

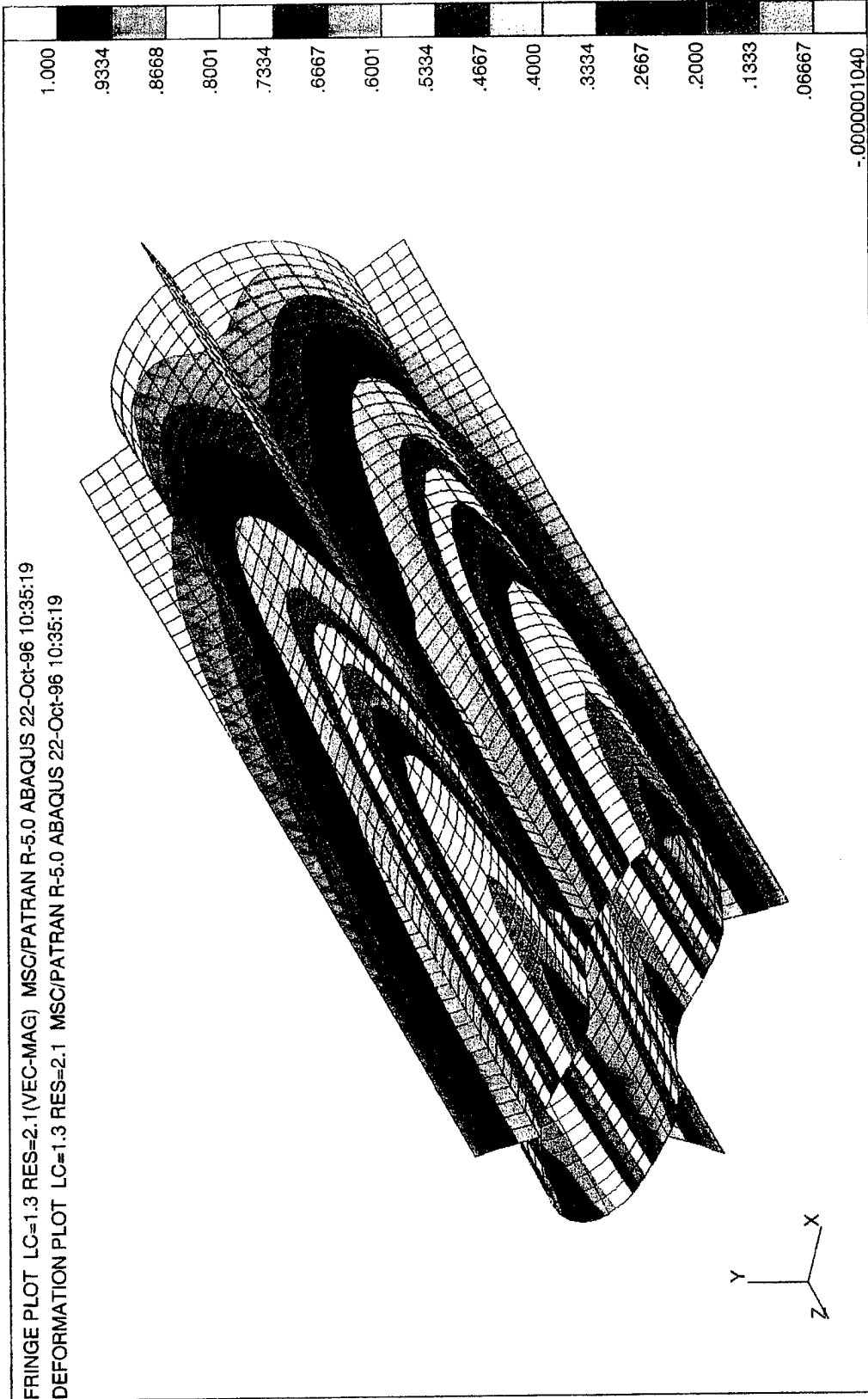


FIGURE 7. MODE SHAPE FOR BUCKLING OF THE UPTAKE

2.2.3 Thermal Stresses in the Uptake

The temperature gradients through the thickness of the uptake walls have the potential to cause very large thermal stresses. The front surface of the steel that is directly exposed to the rocket exhaust will be heated rapidly and try to expand. The material behind the front surface will be at a lower temperature and will resist the expansion of the front surface. The differences in these expansions create thermal stresses within the metal.

Two closed-form models are used to bound the expected thermal stress. The first considers the worst case condition where an extremely thin layer of metal at the front of the wall is heated to a temperature of T_1 . The rest of the material is at a much lower temperature, T_2 . The thin heated layer in front will not be allowed to expand and will be held in compression by the large mass of material at a lower temperature behind it. The magnitude of this compressive stress, σ , is

$$\sigma(T_1) = \frac{\Delta T \times \Delta \alpha \times E(T_1)}{1 - \nu(T_1)} \quad (3)$$

where:

$$\Delta T = T_1 - T_2$$

$$\Delta \alpha = \text{Difference in coefficients of thermal expansion}$$

$$= \alpha(T_1) - \alpha(T_2)$$

$$E(T_1) = \text{Elastic modulus at } T_1$$

$$\nu(T_1) = \text{Poisson's ratio of metal at } T_1$$

The least severe model assumes a linear temperature gradient through the thickness. The compressive stress at the front of the heated surface is

$$\sigma(T_1) = \frac{1}{2} \frac{\Delta T \times \Delta \alpha \times E(T_1)}{1 - \nu(T_1)} \quad (4)$$

This is half the value of Equation (3). The tensile stress at the back wall with a linear temperature distribution is

$$\sigma(T_2) = \frac{1}{2} \frac{\Delta T \times \Delta \alpha \times E(T_2)}{1 - \nu(T_2)} \quad (5)$$

The entrance of the uptake will be subjected to the most severe temperatures. The peak temperature at the entrance to the uptake, T_1 , is predicted to be 2150°F while the back wall temperature, T_2 , is predicted to be 500°F. The material data available for these calculations, however, only go up to approximately 1100°F. As a result, the thermal stresses can only be computed in areas where the peak temperature does not exceed 1100°F.

The peak temperature in the metal is predicted to be 1100°F approximately 28 in. up the uptake. The back wall temperature at this location is 300°F. The properties of A387 Gr 22 class 2 plates at these two temperatures are listed in Table 6. Substituting the values from Table 6 into Equation (3) gives a peak compressive stress of 48 ksi. If a linear temperature gradient is assumed, Equation (4) is used and the peak compressive stress at the front of the metal is predicted to be 24 ksi. The actual magnitude of the stress at the front surface should lie somewhere between 24 and 48 ksi. The yield strength of the steel at 1100°F is only 24 ksi, so there is a good chance the uptake will yield here. Closer to the entrance of the uptake, the temperature gradient will become greater and the peak front wall temperature will increase to 2150°F. Additionally, the yield strength of the metal will decrease. Therefore, it is very likely that the lower section of the uptake will yield during the restrained firing. If yielding occurs, however, the metal will plastically deform and relieve the stresses. Therefore, the maximum stress in the metal due to thermal stresses is equal to the yield strength of the metal. Because of this, according to Reference 7, the first application of thermal stresses cannot cause a structure to rupture. Subsequent applications could cause rupture, though. This is not a problem here because a restrained firing event will not be repeated with the same canister.

TABLE 6. PROPERTIES OF ASTM A387 GR 22 CLASS 2 PLATES AT 300°F AND 1100°F

Property	Temperature = 300°F (T ₂)	Temperature = 1100°F (T ₁)
Coefficient of Thermal Expansion, α	$7.5 \times 10^{-6}/^{\circ}\text{F}$	$9.3 \times 10^{-6}/^{\circ}\text{F}$
Elastic Modulus, E	29 Msi	23 Msi
Poisson's Ratio, ν	0.292	0.31
Ultimate Tensile Strength, S _u	60 ksi	36 ksi
Yield Strength, S _y	35 ksi	24 ksi

Typically, thermal stresses must be added to mechanical stresses to obtain the total stress in a structure. Here, the mechanical stresses caused by the 2 psig steady state internal pressure are 2 orders of magnitude below the thermal stresses and are assumed to be able to be neglected. Thus, the peak stresses in the uptake will not exceed the yield strength of the metal and will not cause catastrophic failure.

The CCL will likely have some permanent deformation in the lower portion of the uptake upon cooling, though. Reference 7 goes on to state that thermal stresses can cause failure by repeated cycling and/or by causing large deflections. The canister will not be reused after a restrained firing so that the first item is not a large concern. The deflections may be minimized by noting that the lower 4 in. of the uptake overlap with the 1 in. thick walls of the plenum. Additional reinforcement is provided by the large flanges between the uptake and the plenum. In the inner cylinder, the first 7 in. are reinforced by a large base plate and an alignment sleeve. These reinforcements will help to hold the structure in place and minimize the thermal deflections. As a result, the deflections may not be noticed until the structure is disassembled.

2.3 ANALYSIS OF THE PLENUM

The flow of the rocket motor exhaust is more complex in the plenum than in the uptake. One-dimensional models are not adequate for predicting pressure in this region. Two- and three-dimensional models are needed instead. These CFD models take a long time to develop. Because of this complexity, the plenum had to be designed without adequate pressure predictions.

Originally, the plenum was designed to withstand 100 psig. This pressure is somewhat arbitrary and was considered an upper limit with an added margin from what the pressures will really be during the restrained firing. The plenum is made with steel walls lined with thick layers of ablative. In the analysis, the ablative is neglected so that the steel wall must carry the entire pressure load on its own.

In addition to analysis, the strength of the plenum will be verified by a hydrotest. The pressure for the hydrotest will be 80 psig. For this test, the plenum will be capped with a 1 in. thick plate that has reinforcements attached.

The plenum is made from A387 Gr 22 Class 2 steel, the same as in the uptake. The properties of this steel were listed in Table 1. Room temperature properties can be used in this analysis because the ablative lining will protect the steel from high temperatures during the restrained firing.

The finite element model of the plenum uses quadratic shell elements and models a quarter section of the plenum. The model used is shown in Figure 8. It consists of a large circular plate that acts as the floor. Attached to this are the walls of the plenum. On the top of the plenum is a flange that is used to connect to a top cover plate during the plenum hydrotest and the uptake during the uptake hydrotest and the restrained firing.

The analysis has been conducted using a 100 psig uniform pressure and symmetric boundary conditions along the edges. Originally, 1/2 in. thick walls were going to be used. This was changed to 1 in. thick to keep the stresses below the 45 ksi yield strength. The Mises stresses predicted in the plenum are plotted in Figure 9. The highest stress occurs near the same fixed bolts that saw the peak stresses in the uptake hydrotest model. The peak stress is 49.6 ksi, slightly above the yield strength of the steel. As with the uptake, the stresses here are most likely overstated.

Aside from the bolts in the top flange, the peak stresses occur at the edges of the flat plates. The Mises stresses in the plenum are plotted in Figure 10 without the top flange to better illustrate this point. The highest stresses occur at the intersection of the floor of the plenum with the walls and the intersection of the octagonal walls with each other. This is a disadvantage of using flat plates instead of a hemisphere. Flat plates under a uniform pressure can develop very large bending moments when their edges are fixed. These moments cause large stresses in the plates. This increases the thickness of the plates needed and increases the weight of the CCL.

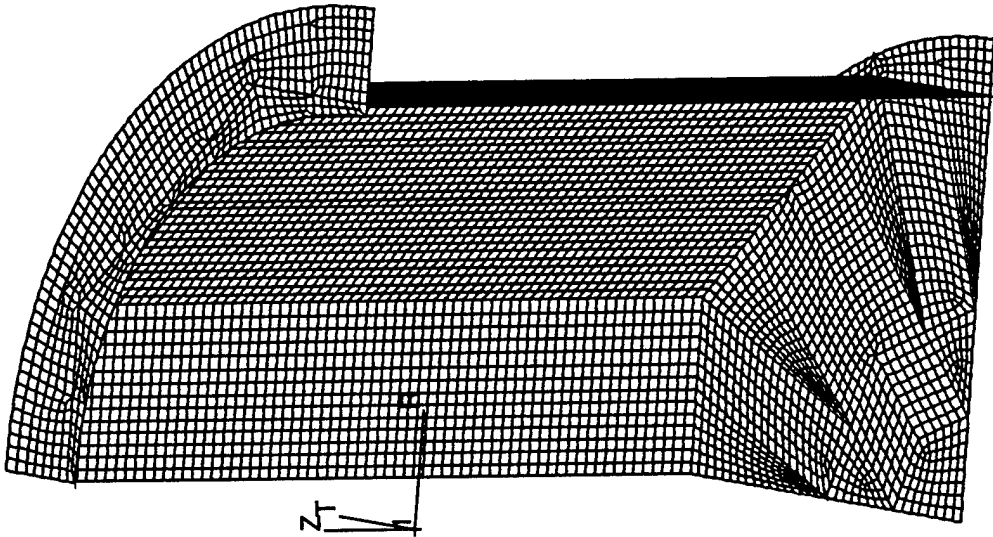


FIGURE 8. PLENUM FINITE ELEMENT MESH



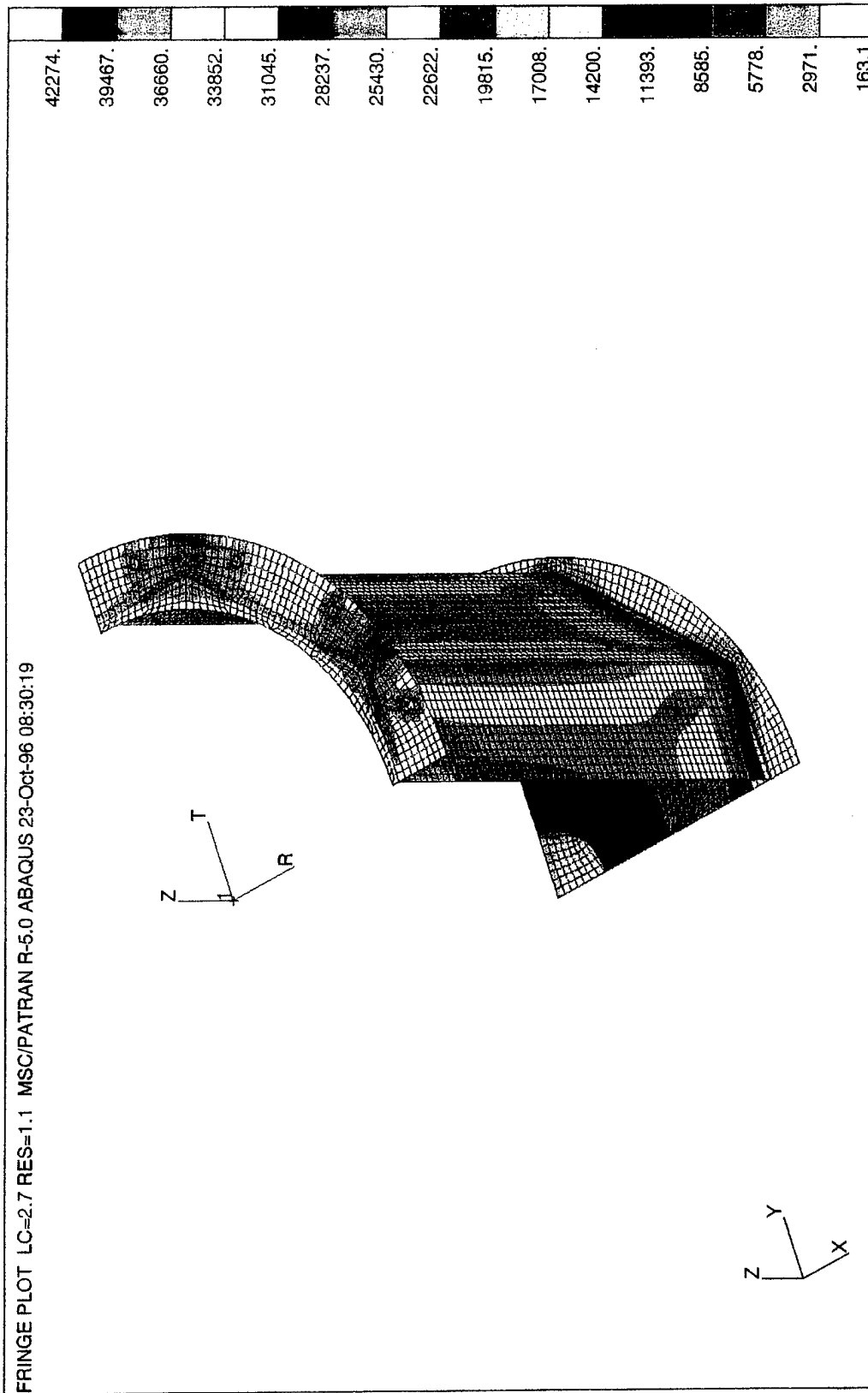


FIGURE 9. VON MISES STRESSES IN PLENUM UNDER 100 PSIG UNIFORM PRESSURE

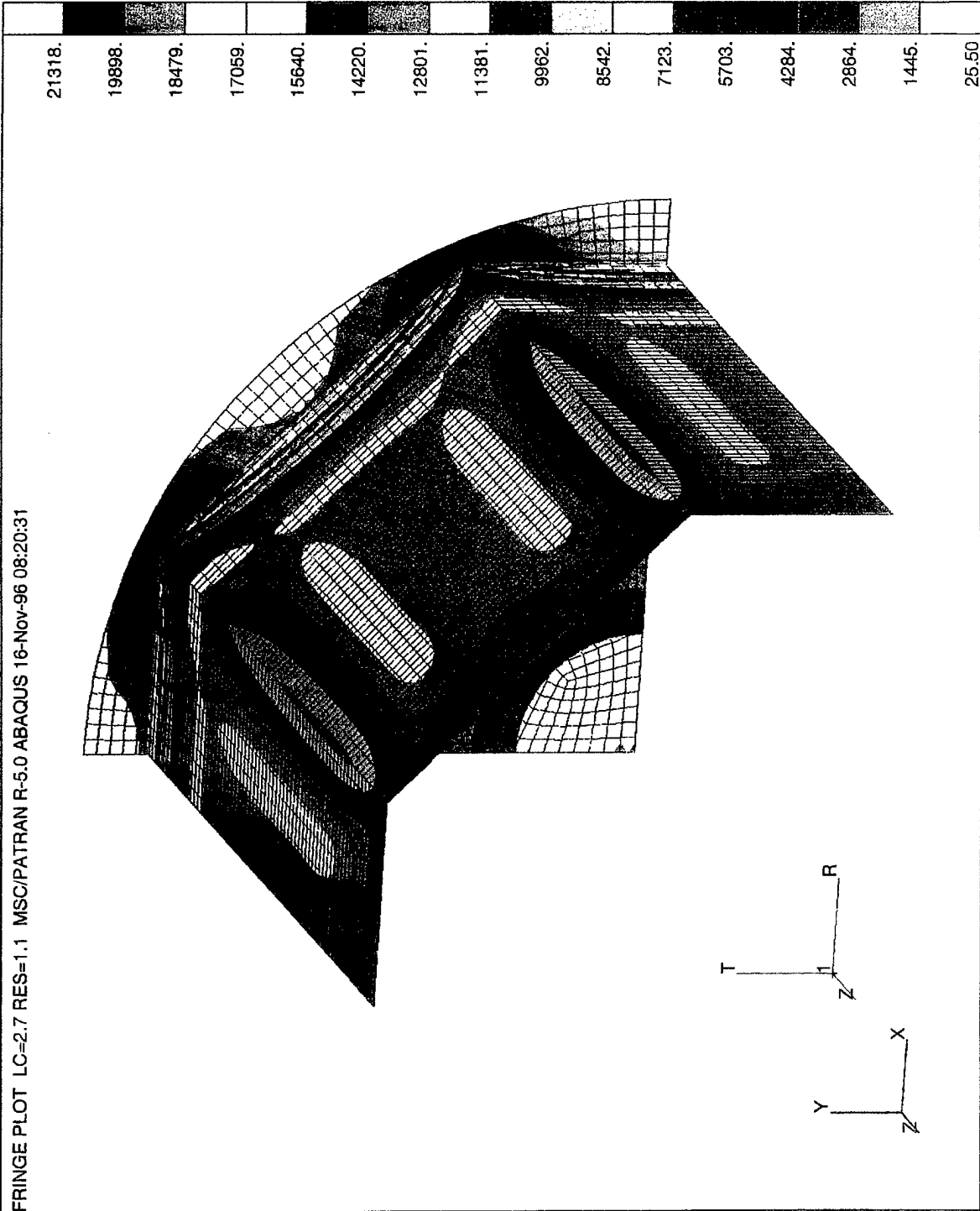


FIGURE 10. VON MISES STRESSES IN PLENUM UNDER 100 PSIG UNIFORM PRESSURE
(WITH TOP FLANGE REMOVED)

To reduce the peak stresses in the top flange, the hydrotest pressure was reduced from 100 psig to 80 psig. The peak stress predicted for each of the plenum components under an 80 psig internal pressure is listed in Table 7.

TABLE 7. PEAK MISES STRESSES IN PLENUM UNDER 80 PSIG INTERNAL PRESSURE

Component	σ_{Mises} (ksi)	F.S. (Using $S_y = 45$ ksi)
Floor	17.4	2.5
Walls	16.0	2.8
Top Flange	23.4	1.9

After the design and the structural analysis of the plenum were complete, 2-dimensional CFD predictions for the plenum pressures became available. The CFD model did not exactly match the geometry of the plenum used in the restrained firing. Instead of being octagonal, it was cylindrical with a flat bottom. Also, instead of being 24 in. deep, the plenum in the CFD model was only 12.8 in. deep. Because of this smaller size, it is assumed that the actual pressures in the plenum will be lower than the pressures predicted here. The 2-dimensional CFD model predicts a peak steady state pressure of 40 psig on the floor and 20 psig on the walls (Reference 8). No predictions have been made for the transient pressures.

If these results are assumed to be correct, the hydrotest pressure will be twice the peak predicted pressure during the restrained firing. The factors of safety that can be expected during the restrained firing are listed in Table 8. Again, this does not include the thick ablative panels that will stiffen the structure and reduce the stresses in the steel.

TABLE 8. PEAK MISES STRESSES IN PLENUM UNDER 40 PSIG INTERNAL PRESSURE

Component	σ_{Mises} (ksi)	F.S. (Using $S_y = 45$ ksi)
Floor	8.7	5.1
Walls	8.0	5.6
Top Flange	11.7	3.8

The stresses in the bolts holding the top plate onto the plenum during the 80 psig hydrotest are checked using closed-form solutions. The top plate used in the plenum hydrotest is 1 in. thick and is reinforced by 1 in. by 4 in. plates. The top plate is assumed not to bend much during the hydrotest because of these reinforcements. If this plate is assumed to be rigid, the only force acting on the bolts connecting it to the plenum will be axial. The magnitude of this external force is equal to the

pressure, 80 psig, multiplied by the area the pressure acts on, 855 in². The external force is 68,400 lbf. The force on each of the 16 bolts, F_e , is 4275 lbf/bolt.

The stresses in the bolts depend on both the magnitude of the external force and the preload in the bolts. To ensure the plenum flange and the top plate don't separate, the minimum preload in the bolts, F_i , should be equal to F_e . The torque needed to produce this force is found using the relation

$$T = cdF_i \quad (6)$$

where c is the torque coefficient (0.20 for unlubricated bolts) and d is the nominal bolt diameter (5/8 in.). The minimum torque, then, is 44.5 ft-lbf.

The recommended preload from Reference 9 should produce a stress equal to 90 percent of the yield strength of the bolt. Grade 5 bolts are assumed to be used. They have a yield strength of 85 ksi. The stress in the bolt due to the preload is

$$\sigma_i = \frac{F_i}{A_t} = 0.90S_y \quad (7)$$

The tensile stress area of the bolt, A_t , is equal to 0.226 in² for 5/8-11 UNC bolts. Equation (7) is solved for F_i to give a preload of 17,290 lbf. The torque needed, then, is 180 ft-lbf. Thus, the torque needs to be between 44.5 and 180 ft-lbf. A torque of 75 ft-lbf satisfies this condition and will be used here.

Now, the total force in the bolts during the hydrotest can be found. Noting that a torque of 75 ft-lbf is to be used, the preload force in the bolt is found to be 7200 lbf from Equation (6). The total force in the bolt, F_b , is equal to

$$F_b = F_{eb} + F_i \quad (8)$$

where F_{eb} is the force in the bolt caused by the external load. This force will be lower than the force that would be created if the preload did not exist. From Reference 10,

$$F_{eb} = \frac{k_b F_e}{k_b + k_p} \quad (9)$$

The total external, force, F_e , is equal to 4375 lbf. The variables k_b and k_p are the spring constants for the bolt and the plate, respectively. The spring constant for the bolts is found from

$$k_b = \frac{A_b E}{l} \quad (10)$$

where A_b is the nominal area of the bolt, 0.3068 in², E is the elastic modulus, 30 Msi, and l is the length, 1.5 in.

From Reference 8, the spring constant of the plate is approximated using

$$k_p = \frac{A_p E}{l} = \frac{2\pi d^2 E}{l} \quad (11)$$

where the area of the plate, A_p , is an area with a diameter 3 times the bolt diameter minus the area of the bolt. The value of k_p is 49.1×10^6 lbf/in.

Using Equation (9), the force on the bolt due to the external load, F_{eb} , is found to be 475 lbf. The total force in the bolt due to both the external load and the preload, F_b , is 7675 lbf. The axial stress in the bolt caused by this force is

$$\sigma_b = \frac{F_b}{A_t} = 34.0 \text{ ksi} \quad (12)$$

The yield strength of the bolt is 85 ksi, so the factor of safety in the bolt during the hydrotest is 2.5.

CHAPTER 3

RESTRAINT OF THE MK 106 BOOSTER

3.1 BACKGROUND

In order to restrain the motor, the heavy-walled TLAM CCL must be able to carry the thrust of the Mk 106. This is accomplished using several restraints that are redundant. The thrust load used in the following calculations is 8370 lbf. This is the peak thrust predicted for a 110°F + 2σ booster. This hot booster should give an upper bound for the actual thrust from the motor during the restrained firing.

3.2 RESTRAINING THE MK 106 IN THE MK 10 CANISTER

The Mk 106 booster is held in place using two large separation nuts that connect to two studs in the aft end of the booster. The separation nuts are tactical except that they will not contain explosive caps for this test. The separation nuts are fastened to the aft end of the Mk 10 canister through a base plate. The nuts are fastened using threaded restraint nuts. Since these components are tactical and already in use, no analysis will be performed on these components.

To reinforce these restraints, a large pipe is fastened to the forward end of the Mk 106. The front of this pipe butts against the test stand. If the restraint nuts, separation nuts, or Mk 10 base plate would fail, this pipe could carry the entire thrust and restrain the motor. The Mk 10 assembly with the secondary restraint attached to the motor is shown in Figure 11. The pipe is analyzed to make sure it can carry the motor thrust considering both compressive and buckling failures.

The axial stress in the pipe is equal to the thrust load, Ft, divided by the cross sectional area of the pipe. The pipe has an outside diameter of 8.75 in. and a wall thickness of 0.50 in. The area of the pipe is 12.96 in². The compressive stress is computed to be 646 psi. The pipe is made from 1026 steel and has a yield strength of 70 ksi. The factor of safety in the pipe under a compressive load, then, is 108. This is extremely high.

Buckling is checked using an Euler beam that is simply supported at the top and allowed to translate, but not to rotate, on the bottom. This model is sketched in Figure 12. The critical load, F_{cr} , that will cause buckling is given by

$$F_{cr} = \frac{\pi^2 EI}{(0.7L)^2} \quad (13)$$

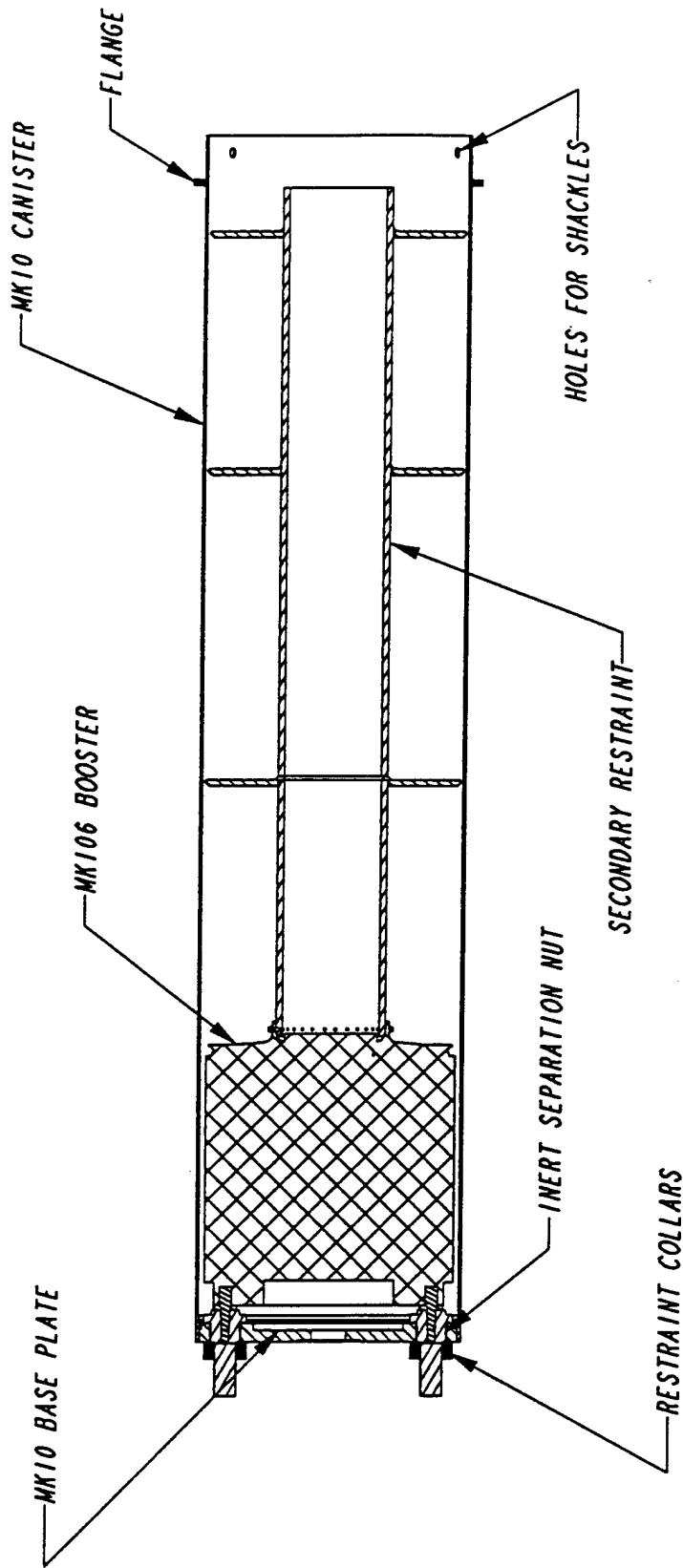


FIGURE 11. MK 10 ASSEMBLY

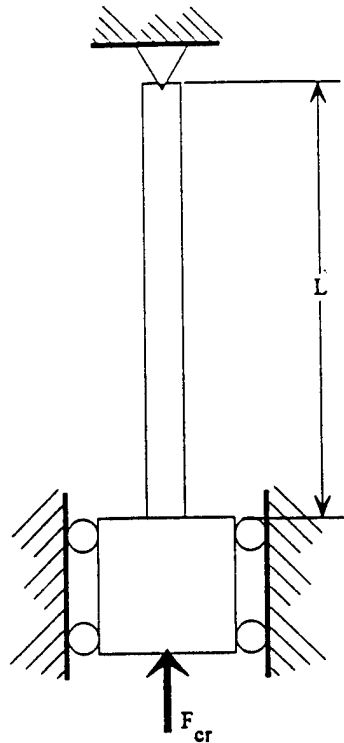


FIGURE 12. EULER BEAM MODEL USED FOR BUCKLING ANALYSIS

The length of the pipe, L , is 67.75 in., the elastic modulus, E , is 30 Msi, and the moment of inertia, I , is 110.7 in^4 . This results in a critical load of $16.1 \times 10^6 \text{ lbf}$ to cause the pipe to buckle. The axial stress in the pipe under this load is 1242 ksi, well above the 70 ksi yield strength of the pipe. Thus, buckling is not a concern.

3.3 RESTRAINING THE MK 10 IN THE CCL

It is just as important to restrain the Mk 10 canister in the CCL as it is to restrain the Mk 106. If the Mk 10 were to let loose while the Mk 106 is still restrained inside, the entire Mk 10 could become a missile. The Mk 10 is restrained at the bottom using the same separation nuts that restrain the Mk 106. At the top, the Mk 10 is held by a flange that bolts into the inner canister. Additionally, the large pipe that attaches to the Mk 106 will help restrain the Mk 10.

The separation nut that holds the MK 106 to the Mk 10 is long enough to fit through a second base plate that attaches to the bottom of the inner canister. An extra pair of restraint nuts have been added below this base plate to hold the Mk 10 in the CCL. The restraints in the bottom of the Mk 106 and Mk 10 are shown in Figure 13.

The stresses in the restraint nuts behind the inner canister base plate have been computed to ensure they can hold the motor. Three modes of thread failure are considered: shear stress in the restraint nut threads, shear stress in the separation nut threads, and bearing stresses between the threads.

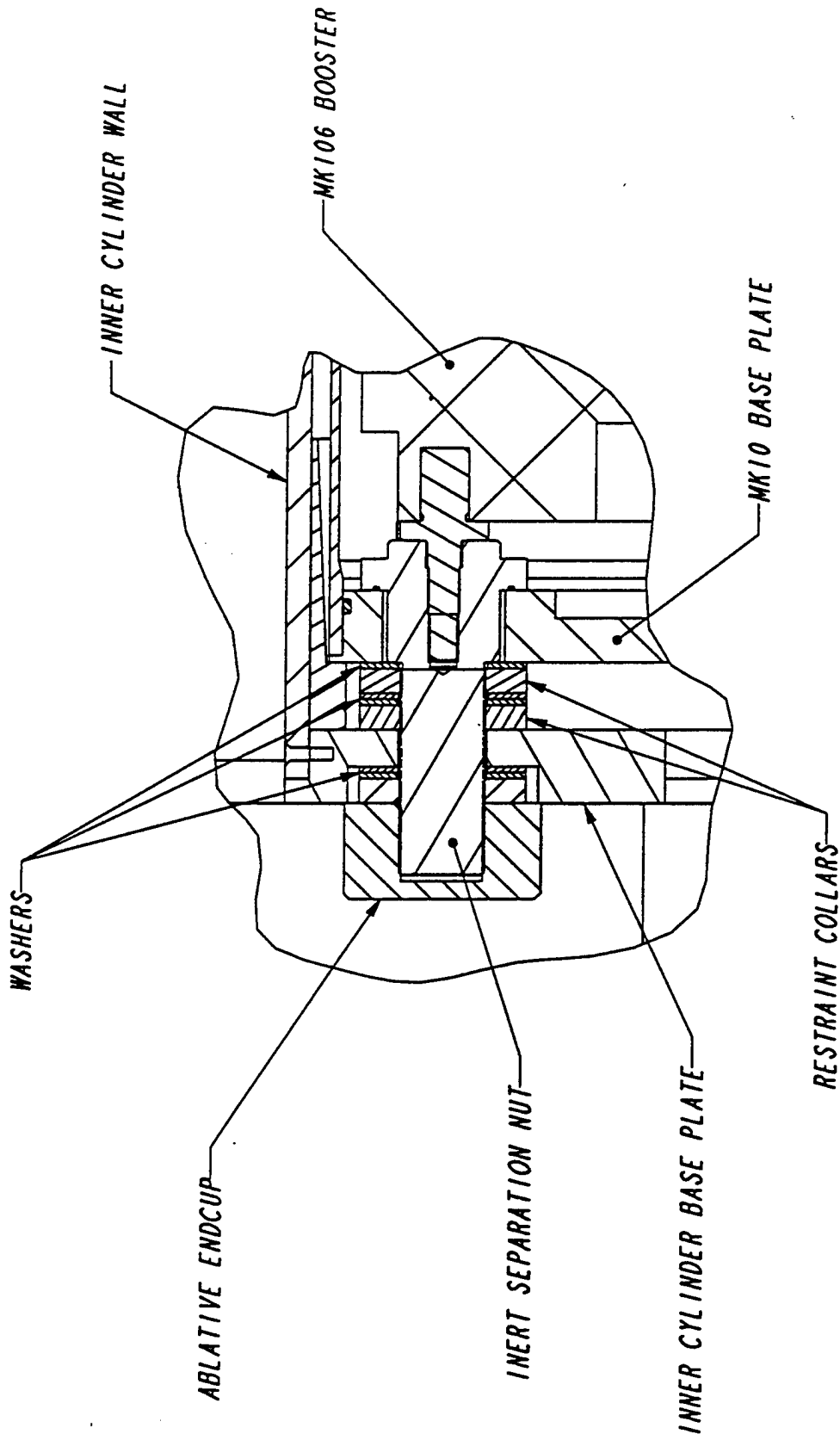


FIGURE 13. LOWER RESTRAINTS FOR MK 106 AND MK 10

The shear stress in the restraint nut threads, τ_n , is

$$\tau_n = \frac{\frac{F_t}{2}}{\pi d \left(\frac{h}{2}\right)} = 3045 \text{ psi} \quad (14)$$

where d is the outside diameter of the bolt, 1.75 in., and h is the thickness of the collar, 0.50 in. Each of the two restraint nuts is assumed to carry half the load, so the thrust force, F_t , is divided by 2. The restraint nuts are made from type 17-4 PH steel and have a yield strength of 170 ksi and an ultimate strength of 190 ksi. The shear strength, τ_y , is half the yield strength, or 85 ksi. The factor of safety with respect to yield, then, is 27.

One risk associated with this calculation (and the following two calculations) is that the temperatures of the separation nuts and restraint collars are not known during the burn. As the temperature rises, the strength of the metal will decrease. As a result, the factor of safety of 27 is likely overstated. However, the factor of safety is so large that, unless the metal were to completely burn through, the threads should still restrain the motor. The yield strength would have to drop from 170 ksi to 6 ksi before the threads will yield. Furthermore, to help minimize temperature effects, the ends of the separation nuts are capped by ablatives.

The shear stresses in the restraint nut, τ_r , are computed using the relation

$$\tau_r = \frac{\left(\frac{F_t}{2}\right)}{\pi d_r \left(\frac{h}{2}\right)} = 3187 \text{ psi} \quad (15)$$

where d_r is the root diameter of the thread, 1.6717 in. The factor of safety here is 26.

Finally, the bearing stresses between the threads are calculated. The bearing stress, σ_b , is found by

$$\sigma_b = \frac{\frac{F_t}{2}}{\left(\frac{\pi}{4}\right)(d^2 - d_r^2)\left(\frac{h}{p_t}\right)} = 2486 \text{ psi} \quad (16)$$

where p_t is the pitch of the threads, 0.0625 in. The factor of safety for bearing stress is 68.

The next item that needs to be checked is the base plate of the inner cylinder. The purpose of this calculation is to make sure this plate will be strong enough to carry the load transmitted to it by the restraint nuts. The plate is made from A387 Gr 22 steel. In this analysis, 1000°F properties are

used. At 1000°F, the elastic modulus, E, and Poisson's ratio are approximately 24.5 Msi and 0.305, respectively. The tensile strength is approximately 53 ksi and the yield strength is 26 ksi (Reference 4).

Several holes in this plate make the calculation of stresses very difficult. Because of this, a finite element model is used. The finite element model has been created using 8-node brick elements. The nodes around the outside edge of the plate, where it connects with the inner cylinder, are fixed. The elements where the collars contact the plate are loaded by a uniform pressure equal to the thrust load.

The deflections predicted in the analysis are plotted in Figure 14. Note that the deflected shape in the figure is exaggerated, since the peak deflection is only 738×10^{-6} in. The Mises stresses predicted by the analysis are shown in Figure 15. The highest stresses occur near the holes and have a magnitude of only 2.99 ksi. The factor of safety in the base plate is 8.7 on yield strength. The primary concern here is that it is likely that some of the plate will burn through. This would most likely occur around the exhaust ports (the two outer 5 in. diameter holes and the center 7.5 in. diameter hole). If this were to occur, it could severely weaken the plate. The potential for localized burn-throughs is one reason the redundancies are needed for the Mk 106 and the Mk 10 restraints.

The Mk 10 is also restrained by a flange at the top. If the base plate were to burn through, this flange would need to carry the entire thrust load. The flange is shown in Figure 11. It is bolted to the top of the inner cylinder by sixteen 1/4 in. bolts. Larger bolts could not be used because of the limited space in this region. Grade 5 bolts are used and have a yield strength of 85 ksi and an ultimate strength of 120 ksi. This region should not be heated much so that room temperature properties can be used.

The stresses in the 1/4 in. bolts will depend upon both the external forces caused by the motor thrust and the internal forces caused by the preload in the bolts. The external force that is applied to each of the sixteen bolts is equal to one sixteenth the total thrust, or 523 lbf. The procedure for finding the stress in these bolts is the same as was used for the 5/8 in. bolts in the plenum cover.

First, the range of allowable torques is determined. The minimum torque is that which will prevent the Mk 10 and inner cylinder flanges from separating. This torque is found to be 2.18 ft-lbf from Equation (6) using a preload value, F_p , of 523 lbf. The recommended preload from Reference 9 is determined using Equation (7) with a tensile stress area, A_t , of 0.0318 in^2 and a yield strength of 85 ksi. This preload is equal to 2433 lbf. The torque needed to achieve this preload is 10.1 ft-lbf. Thus, the bolt torques should be between 2.2 and 10.1 ft-lbf in these bolts. A torque of 5.0 ft-lbf will satisfy this and will still yield an adequate factor of safety when the total stress in the bolt is computed.

With a torque of 5.0 ft-lbf, the preload in each bolt is 1200 lbf. The total force due to the external load is determined using Equations (8) to (10) with a length, l , equal to 0.375 in., an elastic modulus, E, equal to 30 Msi, and a bolt area, A_b , equal to 0.0491 in^2 . This gives a spring constant of 3.83×10^6 for the bolt. The spring constant for the plates, k_p , is different than Equation (11). This joint has a gasket between the metal parts so that the spring constant must be determined using

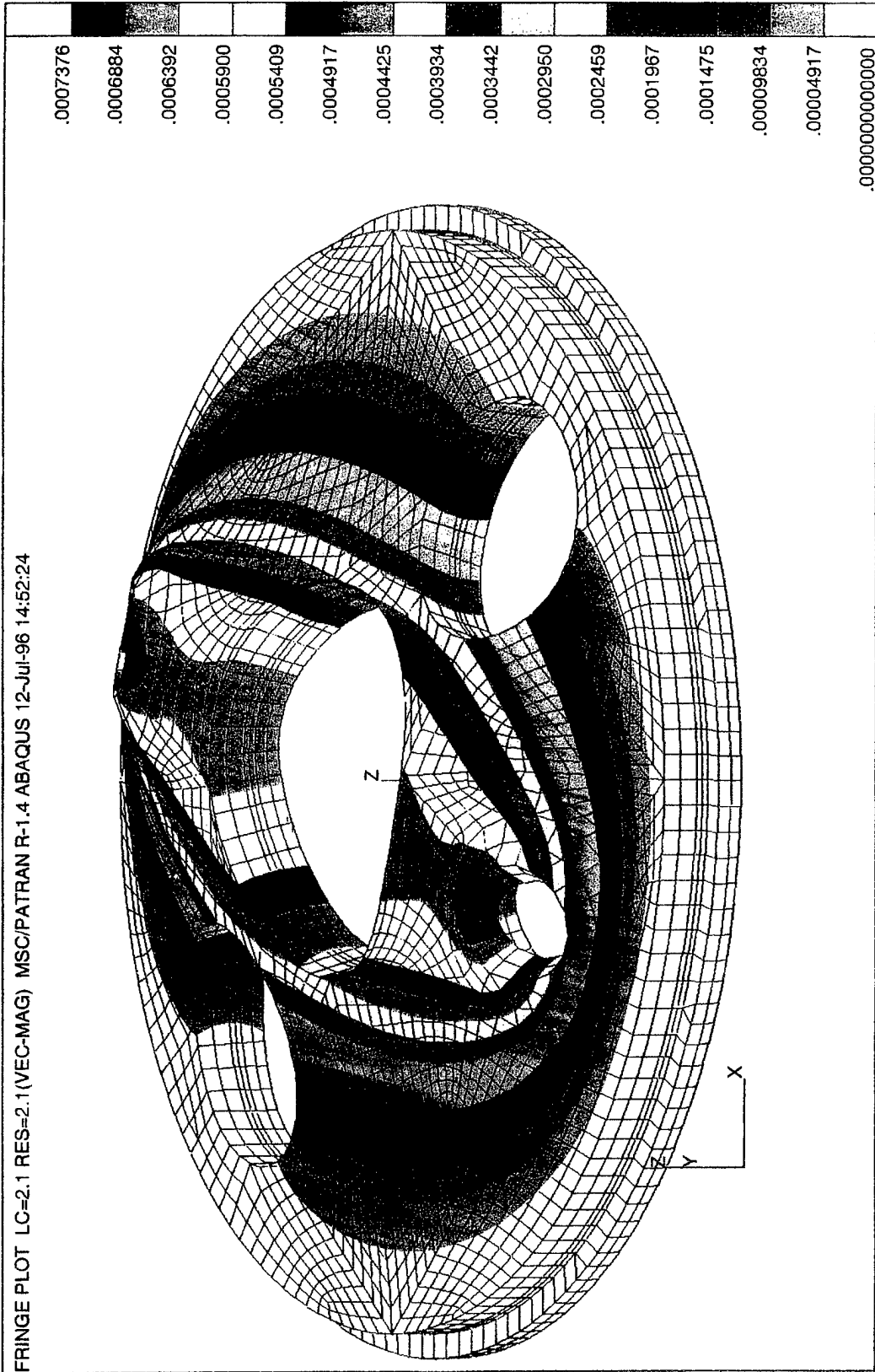


FIGURE 14. DISPLACEMENTS IN INNER CYLINDER BASEPLATE UNDER THRUST LOAD

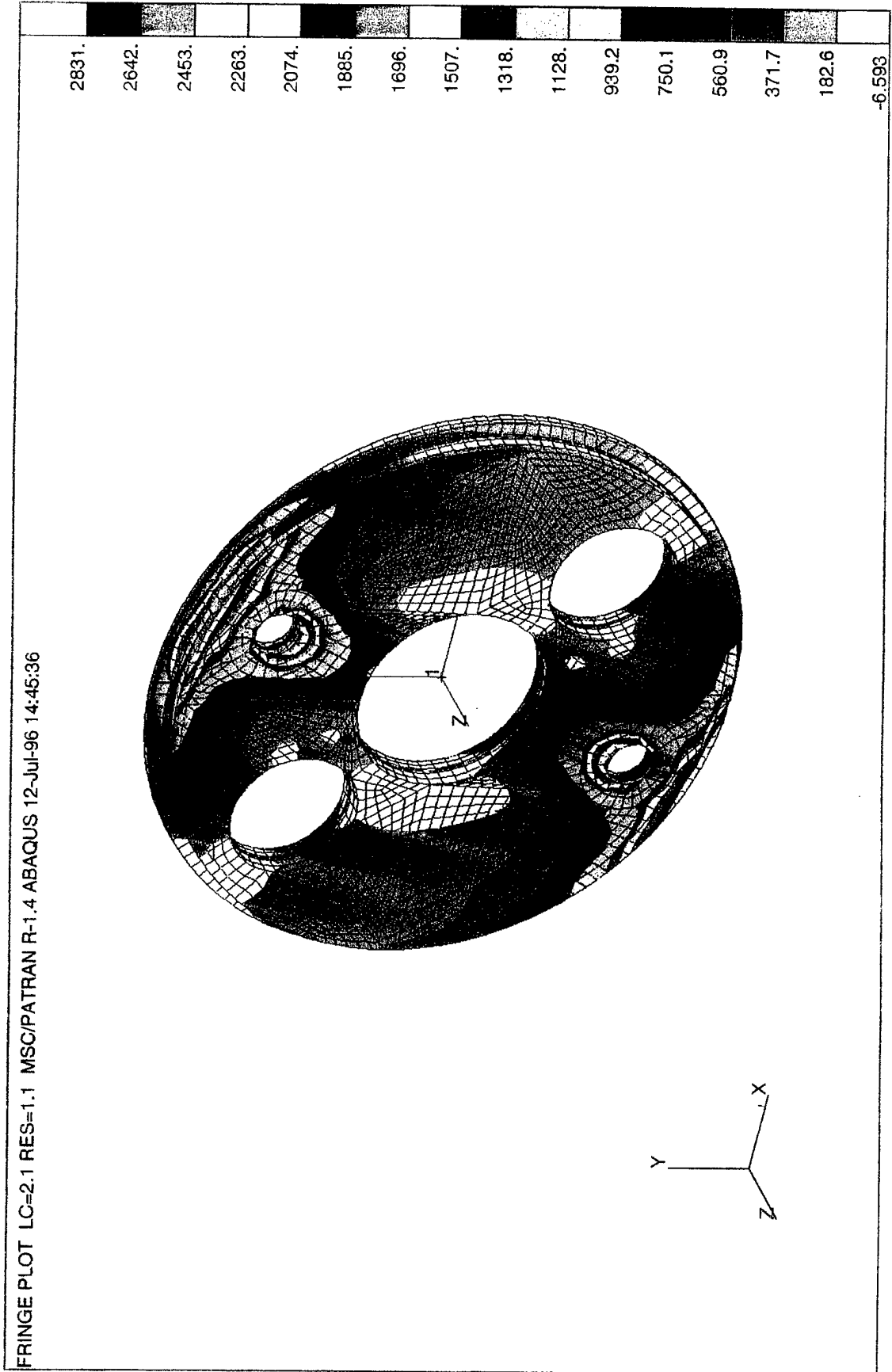


FIGURE 15. VON MISES STRESSES IN INNER CYLINDER BASEPLATE UNDER THRUST LOAD

$$\frac{1}{k_p} = \frac{1}{k_g} + \frac{1}{k_s} \quad (17)$$

where k_g is the spring constant for the gasket and k_s is the spring constant for the steel. The variables k_g and k_s are determined by substituting the appropriate values into Equation (11). For the gasket, E is assumed to be 0.5 Msi and l is 0.125 in. For the steel, E is equal to 30 Msi and l is 0.25 in. Applying these values in Equations (11) and (17) results in a spring constant, k_p , equal to 1.52×10^6 lbf/in.

The external force applied to the bolt is then determined to be 377 lbf from Equation (9) and the total force, from Equation (8), is 1577 lbf. The axial stress in the bolt is then equal to 49.6 ksi under both the preload and the external load. With S_y equal to 85 ksi, a factor of safety of 1.7 is obtained.

As an additional check, the stress in the threads needs to be computed. The bolts in the connection are threaded into the top of the flange of the inner canister. The yield strength of the metal here is only 45 ksi. It is important to make sure the threads in the inner canister will not be stripped by the higher strength bolts.

The shear stress in the internal threads is

$$\tau = \frac{F_b}{\pi d \left(\frac{h}{2}\right)} = 8.03 \text{ ksi} \quad (18)$$

The variable h is the thread engagement length, 0.50 in., and d is the outside diameter of the bolt, 0.25 in. The flange has a shear yield strength of 45 ksi/2, or 22.5 ksi. A factor of safety of 2.80 is computed here. The bearing stress between the threads is

$$\sigma_b = \frac{F_b}{\frac{\pi}{4}(d^2 - d_r^2) \left(\frac{h}{p_t}\right)} = 9.12 \text{ ksi} \quad (19)$$

with the pitch of the bolts, p_t , equal to 0.05 in. and the root diameter, d_r , equal to 0.2012 in. The factor of safety here is 4.9 based on the yield strength of the A387 grade 22 plate (45 ksi).

Thus, the restraint nut, inner cylinder base plate, and the Mk 10's flange are all more than strong enough to carry the rocket thrust and restrain the Mk 10. The weakest link is caused by the axial stress in the 1/4 in. bolts in the top flange in the Mk 10. The factor of safety here is still 1.7. As already noted, all these connections are reinforced by the restraint pipe connected to the Mk 106.

CHAPTER 4

SUMMARY AND RECOMMENDATIONS

4.1 SUMMARY

The structural calculations made here have been used with computational fluid dynamics results to size the components of a heavy-walled CCL. The CFD results documented in References 2 and 3 were used to size the unablated uptake openings to prevent melting of the steel. The rest of the launcher was built around these dimensions. Because this is a test canister, and not a prototype, an attempt was made to over-design the canister. The test will show the feasibility of using an unablated uptake (which can greatly reduce the cost of the canister) and will help to evaluate the erosion, pressures, and temperatures in the CCL. This information will be used to better determine the requirements for a prototype gas management system.

The mechanical analyses consider two primary load sources for the test. These are loads caused by the Mk 106 exhaust gases in the gas management system and by the thrust loads transmitted through the structure by the restrained booster. The exhaust gases create pressure and temperature loads within the structure. The pressure in the uptake is very small and does not stress the structure much. The most critical loads are caused by the heating of the metal. The heating of the metal in the lower portion of the uptake is expected to create thermal stresses high enough to yield the structure. While the high thermal stresses will not cause the uptake to fail, they may cause some permanent deformation in the structure. Also, there is a possibility that there will be localized areas of high heating and erosion in the lower uptake. These were not able to be accounted for in the 1-dimensional CFD calculations used to size the launcher. This is the primary reason the walls of the uptake were made 1/2 in. thick. Additionally, the lower 4 in. of the uptake overlap with the plenum wall to give added protection.

In the plenum, the most critical load is caused by the pressure. An ablative lining in the plenum will shield the structure from most of the heating from the hot exhaust. The pressures from the burn are expected to be less than 40 psig. Nevertheless, detailed CFD results are not available to confirm this. As a result, high factors of safety are used in the design of the plenum. The plenum for this test has 1 in. thick walls. This thickness could be reduced significantly if either a cylindrical or a hemispherical shape were used. Additional reductions in wall thickness could potentially be achieved if better pressure estimates were obtained. This would allow the factors of safety to be reduced.

The motor has several redundant supports to ensure the booster is restrained. Each of these supports is capable of restraining the motor on its own. The primary restraints come from large separation nuts fixed to studs in the aft end of the booster. These are tactical separation nuts used with the Mk 10 canister. The nuts are attached to the CCL through a large base plate. The

mechanical calculations predict factors of safety of at least 8.7 for these restraints. However, this area is directly exposed to the motor exhaust. The amount of damage that the exhaust will cause to these restraints is uncertain. As a result, the other supports for the booster and the Mk 10 canister are at the forward end of the canister, away from the hot gases. The Mk 10 is restrained at the top by a flange that connects it to the CCL. The booster is attached to a heavy pipe that will butt against the test stand. Both supports are more than capable of restraining the booster on their own.

4.2 GENERAL RECOMMENDATIONS

The estimated weights of the various components of the heavy-walled CCL are listed in Table 9. The prototype for the Tomahawk CCL can be made much lighter than the heavy-walled canister. The erosion and temperature measurements from the test will allow the design to be reinforced in critical areas and made lighter in non-critical areas.

To succeed in making the prototype lighter, a greater emphasis needs to be placed on making more detailed analyses of the launcher and on allotting resources to resolving engineering concerns. The design and the capabilities of the design need to be understood in detail before the prototype is built and tested. This includes detailed mechanical design, detailed CFD and structural analyses, and also working with manufacturers to ensure the design can be built economically. In addition to loads from the rocket exhaust, shock, vibration, and handling loads need to be addressed early in the design to avoid costly reworks later. According to Reference 11, "(the) habit of allowing insufficient time for either initial design, or the inevitable re-design, is one of the most common causes of project or product failure." Cutting corners in this phase of the design may appear to reduce short term costs, but will likely result in much higher costs later in the design and/or manufacturing cycle.

TABLE 9. ESTIMATED WEIGHTS OF HEAVY-WALLED CCL COMPONENTS

Assembly	Weight (lb)
Mk 10 Assembly (without booster)	462
Uptake Assembly	3339
Plenum Assembly (including 577 lb of ablative)	2144
TOTAL	5945

4.3 RECOMMENDATIONS TO REDUCE THE PLENUM WEIGHT

The plenum will be able to be made significantly lighter by choosing a different geometry. The plenum used in this test is made from flat plates to form an octagon. This allows standard flat ablative panels to be used and greatly reduces the cost and the time to obtain the ablatives. More efficient shapes for handling pressure could be made from a flat bottomed cylinder or a hemisphere. The

disadvantage of these shapes is that the initial tooling cost for making the ablatives to cover these curved surfaces can be very high. It would have been impractical to create the tooling for this one test. The prototype may very well have a different size than this test canister. This means the molds used to make the ablative for this test could not be reused.

The potential gains from using a flat-bottomed cylinder or a hemispherical dome can be examined using simple closed-form solutions. The circumferential stress in a cylinder is computed using

$$\sigma_c = \frac{pr}{t} \quad (20)$$

where p is the internal pressure, r is the radius, and t is the wall thickness. In the plenum analysis presented in Section 2.3, a factor of safety of 2.8 was attained for 1 in. thick flat plenum walls under a 40 psig internal pressure. If the same material is used for the cylinder, ASTM A387 Gr 22 steel, the yield strength is equal to 45 ksi. The wall thickness needed for a cylinder made from the same material and the same factor of safety can be found by solving Equation (20) for t . The allowable stress, σ_c , is equal to the yield strength divided by the factor of safety, or 16.07 ksi. The radius is 16.5 in. This results in a wall thickness of only 0.08 in., much less than the 1 in. thick walls currently used. Granted, this estimate neglects axial stresses and bending stresses near the end of the cylinder. Also, the floor would still need to be made thicker because it is still a flat surface. However, even if this thickness had to be tripled, the cylinder would still be much lighter than the octagon. The weight of the octagonal plenum is approximately 1567 lbf. A flat-bottomed cylinder with 0.25 in. thick walls and a 1 in. thick floor would only weigh 515 lbf, 1/3 that of the octagonal plenum. (Both weights neglect ablative and include a large flange at the top.)

An even more efficient shape is a hemisphere. Under a uniform internal pressure, the stress in a spherical shell is

$$\sigma = \frac{pr}{2t} \quad (21)$$

Using the same criteria as used for the cylinder, a wall thickness of 0.04 in. is attained. This thickness may be slightly nonconservative because it neglects bending stresses that may exist near the top flange. Even if this thickness is tripled so that a wall thickness of 0.12 in. is used, this geometry represents a significant weight reduction. With this shape a large base plate is no longer needed. The weight of the plenum is now only 100 lbf, 1/15 that of the current plenum.

To determine the optimum plenum geometry, the benefits in weight savings will need to be balanced against the increases in cost. Also, the impacts of the different geometries on the gas flow and heating in the plenum need to be considered in making this determination.

The weights listed above could be reduced further by using a higher strength material. The plenum is ablated, so the metal should not be heated much. Thus, material selection here can be focused on using a high-strength light-weight material without much concern for elevated temperature properties. One caveat is that the plenum material must be compatible with the uptake material so that it will not cause galvanic corrosion.

4.4 RECOMMENDATIONS TO REDUCE THE UPTAKE WEIGHT

The weight of the uptake should be able to be greatly reduced. The radius of the canister and the wall thickness of the uptake are largely driven by the high amount of heating at the entrance to the uptake. These two dimensions were chosen to prevent melting in the uptake.

One significant way to reduce the weight of the uptake is by using a material with better elevated temperature characteristics (especially a higher melt temperature) and/or a lower density. Using a structural material with a higher melt temperature will allow the peak allowable temperature in the metal to be increased. This, in turn, will allow the radius and/or the wall thickness to be reduced. A thorough materials search is needed to identify and evaluate elevated temperature characteristics, density, strength, manufacturability, and cost. Some potential alternatives are austenitic stainless steels and titanium alloys.

Even with a different material, the thermal stresses need to be controlled. The allowable temperatures should not be based solely on the melt temperature of the metal. Thermal stresses can cause the canister to deform under a single application of heat or to burst upon multiple applications. This is especially important if the prototype is designed to be reused and to handle multiple flyouts. The thermal stresses during a flyout must be kept below the yield strength of the metal so that the thermal cycling does not affect the performance of the metal. Also, the temperatures during flyouts must be limited so they do not degrade any heat treatment in the metal.

Weight savings in the uptake can also be achieved by varying the wall thickness of the uptake. The bottom of the uptake experiences the highest temperatures and needs to be thicker. Further up the uptake, the temperature decreases so that this thickness can be reduced. This change in thickness could be accomplished by either tapering the metal or by making the uptake from several sections with different wall thicknesses.

As an alternative to varying the metal wall thickness, the lower portion of the uptake could be ablated. Ablative in the lower portion of the uptake would protect the metal in that region so the walls could be made thinner. Also, ablative material will insulate the structure from the high temperature gradients that cause high thermal stresses. This could be accomplished by putting a short ablated uptake section between the plenum and the unablated uptake. It could also be accomplished by extending the ablated walls of the uptake upward into the entrance of the uptake.

Another item that can be made lighter in the uptake is the longerons. They are currently 1.5 in. thick and could easily be made thinner. Additionally, they do not need to run the entire length of the uptake. It may also be possible to reduce the number of longerons from four to three. This would have to be done carefully because it will increase the potential that the inner cylinder wall could buckle. Reducing the number of longerons would also decrease the strength of the canister under bending loads that can be caused by underwater shock.

CHAPTER 5

REFERENCES

1. Chester, K., *Concentric Canister Launcher, Tomahawk Restrained Firing Evaluation Test Plan*, Naval Surface Warfare Center, Dahlgren Division, Dec 1996.
2. "Restrained Firing of TOMAHAWK Missile in CCL," Naval Surface Warfare Center, Dahlgren Division internal memorandum from G72/Anderson to G72/Keen, 18 May 1996.
3. Basic, J., "One-Dimensional CFD Analysis for TOMAHAWK Restrained Firing Demonstration," NSWCDD Letter Report, Summer 1996.
4. "Elevated-Temperature Properties of Ferritic Steels," *Metals Handbook, Volume 1*, Tenth Edition, ASM International, 1990.
5. Kawada, T., *Data Sheets on the Elevated Temperature Properties of Normalized and Tempered 2.25Cr-1Mo Steel for Pressure Vessels (ASTM A387-D)*, Report 74, National Research Institute for Metals, Tokyo.
6. Young, W. C., *Roarks Formulas for Stress and Strain*, Sixth Edition, McGraw-Hill, 1989.
7. Harvey, John F., *Theory and Design of Pressure Vessels*, Van Nostrand Reinhold, 1985.
8. Informal communication with K. Deloach, Naval Surface Warfare Center, Dahlgren Division/G72, June 22, 1996.
9. Shigley, J. E., *Mechanical Engineering Design*, McGraw-Hill, 1972.
10. Deutschmann, A. D., et al., *Machine Design Theory and Practice*, Macmillan Publishing Co., 1975.
11. Product Design for Manufacturability course notes discussing "Design for Economic Manufacture Strategy," University of Wisconsin-Madison, 1989.

DISTRIBUTIONCopies**DOD ACTIVITIES (CONUS)**DEFENSE TECHNICAL INFORMATION
CENTER8725 JOHN J KINGMAN ROAD
SUITE 0944
FT BELVOIR VA 22060-6218

2

ATTN CODE A76
(TECHNICAL LIBRARY)

1

COMMANDING OFFICER
CSSDD NSWC
6703 W HIGHWAY 98
PANAMA CITY FL 32407-7001**NON-DOD ACTIVITIES (CONUS)**THE CNA CORPORATION
P O BOX 16268
ALEXANDRIA VA 22302-0268

1

INTERNAL

B60 (TECHNICAL LIBRARY)	3
G21 (MILLS)	1
G52 (SETTLE)	3
G64 (MYERS)	1
G64 (THOMAS)	1
G64 (VENTO)	1
G70	1
G704 (YAGLA)	1
G72	1
G72 (BOYER)	1
G72 (CHESTER)	1
G72 (JONES)	5
G72 (KEEN)	1
G72 (LOWRY)	1
G72 (POWERS)	5